Review replies to “The significant role of biomass burning aerosols in clouds and radiation in the South-eastern Atlantic Ocean” by Haochi Che et al.

We would like to thank all reviewers for their constructive comments and suggestions on the manuscript. The feedback has pointed out important aspects that require additional clarity or information and helped us to improve our paper.

In the following, reviewers’ comments are provided in blue, and our responses are in black. Changes to the manuscript made in response to the reviewer are in green.

REVIEWER 1:

In this manuscript, Che et al. run the latest generation of UKESM to investigate aerosol direct, semi-direct, and indirect effects from biomass burning smoke plumes produced by agricultural burning over the southeast Atlantic Ocean. The headline finding (in my read) is that the semi-direct effect of cooling due to increased cloudiness from a stronger cloud-top inversion dominates the overall radiative forcing, offset substantially by the direct effect of smoke absorption and reinforced marginally by indirect effects. The manuscript is well organized and the findings appear sound for the most part. (I do have some questions below, mainly pertaining to the Twomey effect). The text could use some areas of clarification and potentially additional information. I would not anticipate any major new analyses would need to be undertaken to address my comments, so I therefore recommend publication following minor revisions.

Thanks for the positive feedback! Significant reversions have been made to improve the clarity of the manuscript based on the comments from both reviewers.

General comment:

My biggest (really, only) concern with the results is that the indirect effect estimate seems unrealistically small given the change in cloud droplet number concentration you diagnose. From a simple back-of-the-envelope calculation of the Twomey effect, a doubling of cloud droplet concentration (you report 56% of CDNC are from biomass burning) should lead to a radiative forcing of O(10) W/m2, as in Lu et al. (2018). This is before taking into account the small liquid water increases you find. In my own work in the region (Diamond et al., 2020), I’ve estimated that a 5% increase in climatological CDNC from the influence of shipping produces a radiative forcing of ~-2 W/m2 during austral spring. I thus find it hard to believe that doubling CDNC would produce less than that in austral winter.

We thank the reviewer for pointing this out. This is actually a misunderstanding due to the inaccurate expression. The CDNC increased by the BBA is **up to** 56% only in some specific areas, not the average. We have calculated the mean contribution of BBA to CDNC during July and August in the SEA domain (the area this paper focuses on, ranging from 30° S to 10° N and from 40° W to 30° E), and the result shows the mean CDNC increase by BBA is around 13% and around 1.1% in the cloud box region. Although the indirect radiative cooling associated with the changes of CDNC is smaller than that in Diamond et al., (2020), some differences are to be expected taking significant model differences into account.

To avoid confusion, we have revised the manuscript as follows:

Though BBA can contribute up to 56% of total CDNC in some areas, its average contribution during July to August in the SEA is around 13%, much less than its contribution to the $CCN_{0.2\%}$ budget fraction.

Specific comments:

1. Title: The title is currently rather non-informative. I would recommend highlighting that the semi-direct effects dominate (really the highlight of the paper in my opinion) in the title, and also mentioning that this is a global climate modeling study (as opposed to in situ or satellite observations or high-resolution process modeling).

Agree. Both reviewers have suggested to make the title more specific. According to the comments, the title has now changed to:

Cloud adjustments dominate the overall negative aerosol radiative effects of biomass burning aerosols in UKESM1 climate model simulations over the south-eastern Atlantic

2. Page 2, Line 1: I don't follow why the net sign of the aerosol radiative effect, rather than its magnitude, signifies the importance of aerosol in this region.

The net negative radiative effect of biomass burning aerosol results from the strong cooling of the semi-direct effect. Therefore, this sentence has been deleted, and the previous sentence has been revised as the following to underline the importance of the semi-direct effect.

Among the effects of biomass burning aerosols on the radiation balance, the semi-direct radiative effects (rapid adjustments induced by biomass burning aerosols radiative effects) have a dominant cooling impact over the SEA, which offset the warming direct radiative effect (radiative forcing from biomass burning aerosol-radiation interactions) and lead to overall net cooling radiative effect in the SEA. However, the magnitude and the sign of the semi-direct effects are sensitive to the relative location of biomass burning aerosols and clouds, reflecting the critical task of the accurate modelling of the biomass burning plume and clouds in this region.

3. Page 3, Line 3: I would argue that in situ results showing abundant biomass burning influence within the MBL at Ascension Island from the LASIC campaign (Zuidema et al., 2017) and throughout the SE Atlantic Klein-Hartmann box over the remote ocean from ORACLES (Diamond et al., 2018; Kacarab et al., 2020) are more directly relevant to your point about smoke-cloud interaction.

Thanks for the suggestion! We have adapted the comments and included the papers by Zuidema et al. (2018), Diamond et al. (2018), and Kacarab et al. (2020), in our manuscript.

However, recent studies found abundant biomass burning influence within the marine boundary layer (MBL) at Ascension Island from in-situ observations (Zuidema et al., 2018) and throughout the SEA from flight measurements (Diamond et al., 2018; Kacarab et al., 2020), confirming the interaction of BBA and clouds.

4. Page 3, Line 5: I don't believe the cited literature backs up the claim that "most" of the BBA is entrained into the MBL.

This sentence has been deleted, as the plume-cloud interaction has been described in the above text.

5. Page 3, Line 24: The large eddy simulation results of Yamaguchi et al. (2015) and Zhou et al. (2017) also seem relevant to cite/discuss here.

Agree, the sentence has been revised as:

Hence, related process studies mainly rely on high-resolution limited-area models (Gordon et al., 2018; Lu et al., 2018), as well as idealised large-eddy simulations (Yamaguchi et al., 2015; Zhou et al., 2017)

6. Page 4, Lines 1-2: The BBA plume subsiding and gradually meeting the rising MBL is true in the mean, but the picture is much more nuanced in reality, as instances of smoke-cloud contact were seen to be highly variable between and even with flights during the ORACLES and CLARIFY campaigns. It is also not necessarily the case that smoke-cloud contact corresponds instantaneously with the MBL being polluted, as discussed in Diamond et al. (2018).

Agree, we acknowledge that although the MBL is mostly polluted with BBA at Ascension Island (Zuidema et al., 2018), in other instances, the MBL is relatively clean, as influenced by the recirculation. However, around Ascension Island, both ground-based and flight observations have confirmed the frequently observed BBA (Zuidema et al., 2018, Wu et al., 2020). Therefore, it is reasonable to presume BBA have generally reached the MBL near Ascension Island. We also agree that even with the BBA entering the MBL; cloud properties are not affected by the instantaneous smoke-cloud contact, as discussed by Diamond et al. (2018). Therefore, to make it clearer, we have made the following revision:

These flight campaigns were carried out during the biomass burning seasons, and have provided an ideal dataset covering both BBA above and interacting with clouds, as previous studies have found that the BBA plume layer generally subsides and meets the gradually deepening marine boundary layer in the vicinity of Ascension Island and St Helena (Adebiyi et al., 2015). However, observations also indicate that the entrainment of BBA into the MBL can be intermittent, can require significant contact time (Diamond et al., 2018), and that recirculation patterns can result in clean MBL near Ascension Island.

7. Page 4, Line 13: Is dust included as one of the “five interactive log-normal aerosol modes”? I only count four other components (sulfate, sea salt, black carbon, organic carbon). The phrasing currently is confusing, as it sounds like the dust representation is entirely separate.

In this model configuration, dust is not included in the modal GLOMAP microphysics; it is treated separately in the model using a 6-bin externally mixed scheme(Woodward, 2001), while the interactive log-normal distribution simulates sulfate, sea salt, black carbon, and organic carbon. The “five interactive log-normal aerosol modes” in the manuscript refer to the modal aerosol modes (4 Soluble from nucleation to coarse and one insoluble of Aitken mode), not the aerosol species. The aerosol species are internally mixed in each mode. To avoid confusion, we have made a revision as below:

Aerosol and its interaction with clouds are represented by the UK Chemistry and Aerosol model (UKCA) (Mulcahy et al., 2020; O’Connor et al., 2014), including the modal aerosol microphysics GLOMAP (Mann et al., 2010), with five interactive log-normal aerosol modes (four soluble modes from nucleation to coarse, and one insoluble Aitken mode) comprised of internally-mixed sulfate, sea salt, black carbon, and organic carbon. Mineral dust is represented separately by an externally mixed bin representation (Woodward, 2001).

8. Page 5, Line 9: Somewhere in the manuscript you should discuss the implications of only looking at one part of the biomass burning season (July-August). It is well known that the BB plume properties change over the course of the biomass burning season, influenced in part by meteorological shifts like the strengthening of the southern African Easterly Jet (AEJ-S) in September and October that corresponds with a more elevated plume (Adebiyi & Zuidema, 2016).

Thanks for the suggestion. The corresponding discussion has been added as below:

Two years are simulated in the model (2016 and 2017), however this analysis focuses on July and August, for consistency with the flight campaigns. Note although July and August can be used to represent BBA effects during the African fire season (July-October), this selection will also result in some uncertainties, as the BBA distribution and properties change over the course of the fire season, influenced in part by meteorological shifts, such as the strengthening of the southern African Easterly Jet (AEJ-S) in September and October, corresponding to a more elevated plume (Adebiyi and Zuidema, 2016).

9. Page 5, Lines 17-20: I'm surprised that you do not use any of the new products from MODIS or SEVIRI that account for above-cloud aerosol absorption. I would recommend trying the comparison using one of those products or at least discussing the issues with traditional AOD products that cannot retrieve AOD in the presence of clouds.

The primary model evaluation is done by comparing extinction measured from ORACLES and CLARIFY flights with the model. The MODIS AOD is used to validate the model bias in simulating the BBA plume after the evaluation. The model has been collocated with the MODIS AOD to reduce uncertainties (Schutgens et al., 2016). Although the AOD we used in the manuscript is the traditional product from MODIS, it is comparable with the model, after the collocation.

The main purpose of the AOD comparison is to evaluate the plume simulated in the model. The standard MODIS AOD retrieval is well evaluated and documented, although at Ascension Island, mean AOD (2001–2018) is slightly overestimated (around 0.02) by the MODIS (Gupta et al., 2020). However, the experimental nature of the above-cloud retrievals could be an issue, and require a very careful consistent determination of "above cloud", which is not always trivial in a climate model.

10. Figure 1: What altitude is being shown, or is this a column average? There is a large amount of vertical variability in the plume (as seen in Figure 2) so the 2D picture is a bit difficult to interpret.

This is the collocated model extinction, i.e., the extinction from the model is at the same time, latitude, longitude and altitude as the flight data. Thus, the comparison is point to point. To make it clearer, we have changed the figure caption as below:

Figure 1: Mean along track aerosol extinction coefficient [Mm^{-1}] from the (a) UKESM1 model collocated to the flight tracks, (b) flight observations, and (c) differences between the model and observations. Note that the model extinction is under ambient conditions, whereas the measured extinction is for dry aerosols with relative humidity below 30%.

11. Page 6, Line 4: I do not understand why you only compare September AOD when the analysis focuses on July-August. As discussed earlier, there are known differences in plume location throughout the biomass burning season, in part driven by different meteorological factors between July-August and September-October. Thus, it's entirely possible that the model could represent one part of the season well but the other poorly if it is not representing those meteorological shifts properly. Figure S2 should be replaced with a new version including July and August.

We have changed the figure as illustrated below. The figure now shows the comparison of the mean AOD from model and MODIS (Terra and Aqua) from July to August, 2016-2017.

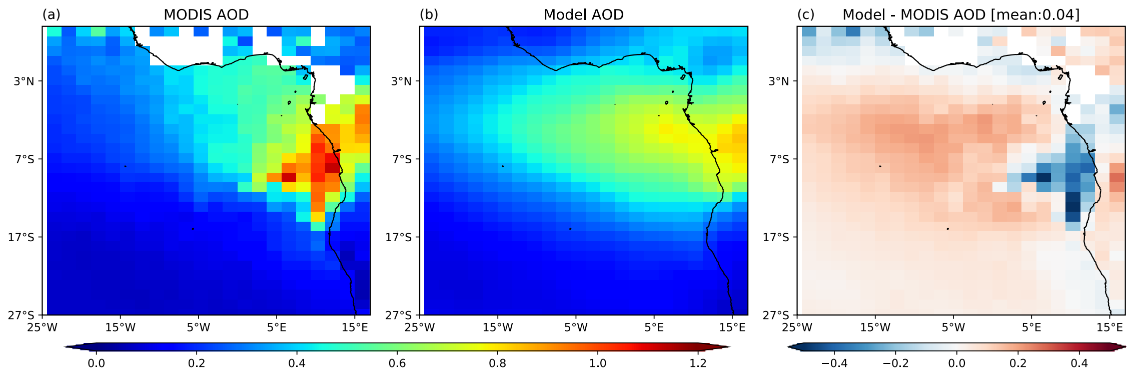

Figure S2. Mean (a) MODIS and (b) UKESM1 simulated AOD during July and August 2016-2017, and the (c) differences between MODIS and the model.

12. Page 6, Lines 12-13: As discussed above, although this description makes sense in the climatology, the picture we found in the field is much more complicated than the mean suggests. For one, much of the smoke in the marine boundary layer at a given location may have been entrained upstream and not necessarily reflect the properties of the plume above-cloud at the time of sampling (Diamond et al., 2018). It may be worth noting that although the mean field shows a plume subsiding from east to west, actual plume distribution and occurrence of plume-cloud contact at any given time is more nuanced.

This is similar to question 6. We agree that even when BBA enter MBL, cloud properties will not be affected by the instantaneous smoke-cloud contact as discussed by Diamond et al. (2018). Therefore, to make it clearer, we have made the following revision:

From east to west, the plume subsides and comes into contact with the clouds. At 5° W, the plume is generally inside the clouds, although the actual plume distribution and occurrence of plume-cloud contact at any given time can be more nuanced (Diamond et al., 2018). Thus, the BBA can interact and modulate cloud properties. This finding is also confirmed by previous studies (Adebiyi et al., 2015; Chand et al., 2009; Deaconu et al., 2019; Gordon et al., 2018).

13. Page 7, Lines 6-7: Are these percentages for the column burden? It may be worth also reporting the values for the marine boundary layer separately (if they differ), as the MBL CCN concentration is what matters most for cloud droplet activation.

Yes, these are percentages of the column burden CCN. We agree that the marine boundary layer CCN is more important in affecting cloud droplet number concentration. The CCN concentration and fraction are indeed quite different in MBL, we have a manuscript under preparation discussing the CCN source attribution, and find the mean number concentration of the BBA $CCN_{0.2\%}$ during biomass burning season is ~75 cm^{-3} in the MBL and ~209 cm^{-3} in the plume layer. The BBA $CCN_{0.2\%}$ fraction is ~40% in the MBL and ~84% in the plume layer, during the BB season. The detail of the CCN distribution will be discussed in the upcoming paper.

14. Figure S3: Figure S3 is an exact copy of Figure 3. I believe the figure the authors meant to include would show the change in CCN due to BBA?

Figure S3 shows the spatial and vertical distribution of total CCN, while figure 3 is the CCN from biomass burning. These two figures share the same pattern, indicating biomass burning is the main source of the CCN. We have changed figure S3 as below, to show the fraction of biomass burning CCN. Although the updated figure still has the same pattern as the CCN from BBA, which highlights the contribution of BBA to CCN.

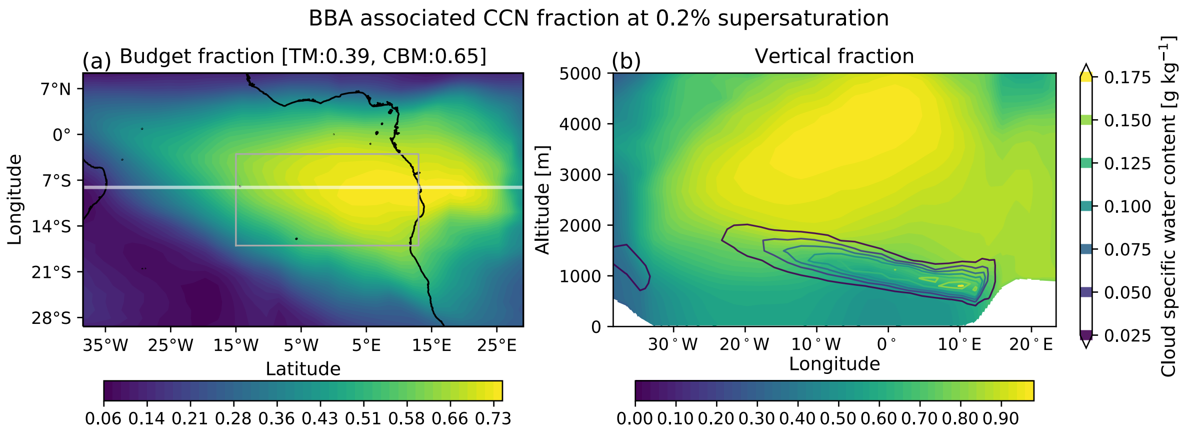

Figure S3. UKESM1 simulated mean fraction of CCN from BBA at 0.2% supersaturation under standard conditions for temperature and pressure (STP) during July and August 2016-2017 as (a) the fraction of vertically integrated burden and (b) fraction of profile along the latitude of Ascension Island, 8.1° S (the white line in Fig. 3a). The domain in Fig. 3a, ranging from 30° S to 10° N and from 40° W to 30° E, is the focus area of this paper. The grey box in the map (cloud box) representing the cloudy areas where the averaged low cloud fraction is above 0.58. The TM is the total mean of the domain, and the CBM is the mean of the cloud box. The contours in Fig. 3b is the cloud specific water content in the baseline simulation.

15. Page 7, Line 27: This should be testable by looking at the average strength of the cloud-top inversion between the different model runs directly.

We have added the variation of the temperature profiles in the supplement to show the strengthening of the cloud-top inversion, as below:

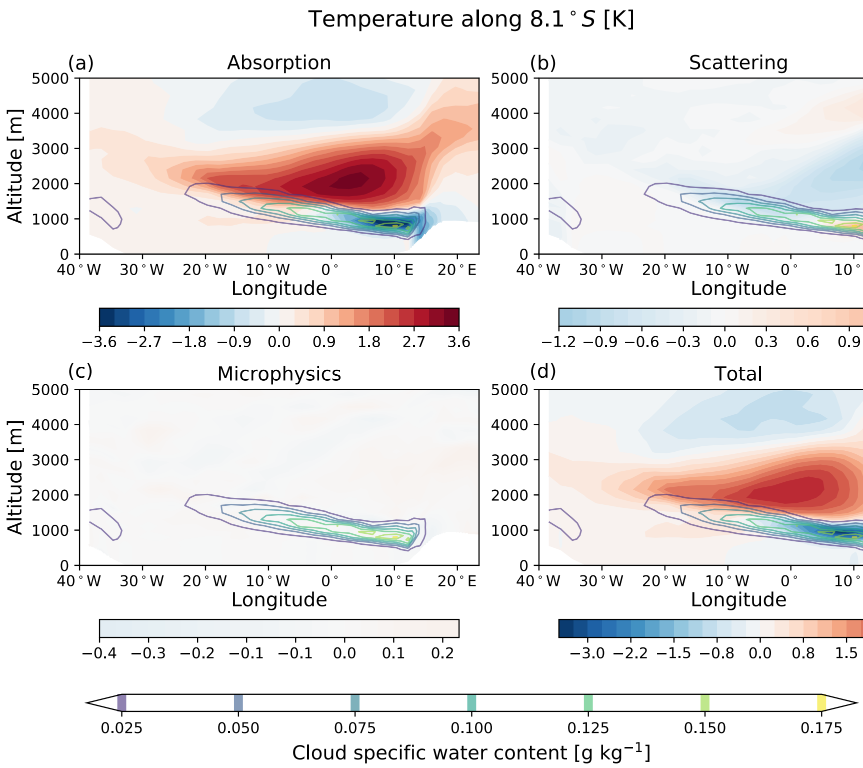

Figure S5. UKESM1 simulated mean vertical profiles of the BBA effects (a) absorption, (b) scattering, (c) microphysical and (d) total on temperature along the latitude of Ascension Island (cf. Fig. 3a) during July and August, 2016-2017. Contour lines represent baseline cloud specific water content. The same colourmap scale is used in each plot to facilitate comparison, but the colourmap ranges differ in each plot, corresponding to the maximum and minimum of temperature at each.

16. Page 8, Line 4: This statement needs qualification, as the SS increases where most of the cloud mass is. Are you only referring to the westernmost region? Or this actually supposed to say that the increase in SS is noticeable in the net (decrease from microphysics is more than compensated by increase from absorption)?

Thanks for the correction. This was a mistake as it should be "increase" not "decrease". The increased SS is noticeable in the net near the continent and at the lower altitude, as the decrease from microphysics effect is totally compensated by the increase from absorption effect. Therefore, the net SS has a similar pattern with the absorption effect in this area. We have changed the sentence as below:

The increase in the maximum supersaturation from the BBA total effect is still quite noticeable.

17. Page 8, Line 20: BBA being 56% of the CDNC is less than the 68% figure quoted above for CCN, but is that for the column or MBL only? It would be more relevant to compare the fraction of MBL CCN that is from BBA to the CDNC change, as the BBA aloft does not activate.

BBA contributes up to 56% of CDNC, while this contribution only happens in some areas. The average contribution of BBA during July-August in the SEA is around 13%. The increased CCN is a column budget. We acknowledge that the CCN in the MBL is more relevant, and it a CCN source and budget analysis is the topic of a manuscript in preparation. We have revised the sentence and made it clearer that the free troposphere CCN would also contribute to the high fraction of CCN. And we also deleted the sentences discussing the supersaturation and particle diameters.

Though BBA can contribute up to 56% of total CDNC in some areas, its average contribution during July-August in the SEA is around 13%, much less than its contribution to the $CCN_{0.2\%}$ budget fraction. This indicates a contribution of BBA above the cloud layer, unable to activate, although they can serve as CCN at 0.2% supersaturation.

18. Page 8, Line 30: The various LES studies cited in this review (Yamaguchi et al., 2015; Zhou et al., 2017) and by the authors (Herbert et al., 2020) seem relevant to reference here in addition to the classic study of Johnson et al. (2004).

Thanks for the suggestion! We have added the corresponding references.

This finding is consistent with the result of large-eddy simulations researches (Herbert et al., 2020; Johnson et al., 2004; Yamaguchi et al., 2015; Zhou et al., 2017) that above cloud BBA can inhibit cloud-top entrainment and increase LWP.

19. Page 8, Line 33: This is due to the absorption effect lowering the relative humidity within the MBL, correct? It would be helpful to be explicit about this.

Yes, when the BBA is inside the MBL, it could reduce cloud droplet numbers by lowering the relative humidity. We have revised this sentence as follows:

When BBA is transported further from the continent, the entrainment of BBA into the cloud layer reduces cloud droplet numbers by lowering the relative humidity through diabatic heating from absorption, which further reduces the increase of LWP, and results in a nearly zero or slightly negative effect on LWP.

20. Page 9, Lines 2-3: The LWP effect of BBA absorption is to increase LWP as one moves from west to east. The text is written to make it sound as if LWP is decreasing from west to east due to BBA absorption. The text should be clarified here.

We have rewritten this sentence in below:

The increased LWP from BBA absorption is mainly located near the continent where the BBA and clouds are well separated, indicating the role of BBA in modulating the cloud distribution.

21. Page 9, Lines 16-17: You should clarify that the BBA in the MBL suppresses CDNC through the semi-direct effect here, not the indirect effect (which actually causes CDNC to increase substantially).

We have made the corresponding change:

However, when more BBA are entrained into the MBL, the BBA decrease the number of cloud droplets through its absorption effect and therefore have a negative impact on the cloud albedo.

22. Page 9, Lines 23-24: As mentioned in the general comment, this result is very surprising given the large increase in CDNC, which should lead to an albedo increase of ~0.05-0.10.

This has been discussed in the response to the general comment. We have calculated the average CDNC in the SEA, and results show that the CDNC increased by BBA is around 13% on average; while in the cloud box region, this number is only around 1.1%.

23. Page 10, Line 3: I don't understand how the indirect effects could have led to a warming given both CDNC and LWP increase. Did cloud fraction decrease anywhere? Or could this just be due to weather noise between different initializations?

We have checked the cloud fraction, and it is increased by the microphysics effect. The warming "indirect effect" occurs mainly in the shortwave, while the cloud fraction and LWP both increase. Therefore, the increase of the indirect effect is likely due to the weather noise between different simulations. We have made the following revision:

In some areas, the indirect effect shows a slight warming effect, which may be caused by the weather noise unconstrained by nudging between different initializations, as the cloud fraction and LWP both increase.

24. Page 10, Lines 20-21: This sentence should be rewritten for clarity. The semi-direct effect is not cooling at cloud top and warming below; rather, above-cloud semi-direct effects lead to a TOA cooling whereas below-cloud semi-direct effects lead to a TOA warming.

As the reviewer suggested, we have revised the sentence as below:

However, in our simulation, the BBA plume is not well separated from the underlying clouds. Thus, when the BBA are closer to the cloud, some BBA may have entered the cloud layer. As a result, the above-cloud semi-direct effects lead to a top-of-atmosphere (TOA) cooling, whereas in-cloud semi-direct effects lead to a TOA warming.

25. Page 10, Line 29: The results of Gordon et al. (2018) are also averaged over a different region that you are using, correct? It would be helpful to compare the values averaged over the same region, as the spatial mismatch could also lead to discrepancies.

Yes, Gordon et al. (2018) used a different domain. We have re-calculated the radiative forcing in the domain studied in their paper and found their direct and semi-direct effects are roughly two times higher than ours, which may be because they only averaged the five most polluted episodes. In contrast, the indirect effect is still quite different and un-proportional, as they have an assumed higher kappa of the OC. The manuscript has been revised as follows:

Comparing the radiative effects in the same domain, the direct and semi-direct effects from their simulations (direct effect: 10.3 Wm^{-2} and semi-direct effects: -16.1 Wm^{-2}) are roughly two times higher than our results (direct effect: 3.3 Wm^{-2} and semi-direct effects: -9.2 Wm^{-2}), as they only sampled the five most polluted days during their simulations. Nevertheless, the indirect effect in their results is -11.4 Wm^{-2}, which is disproportionately higher than our simulation (-0.6 Wm^{-2}). The possible reason behind this discrepancy is that the OC kappa value in their simulation is 0.88, which is much higher than our setting of 0.3.

26. Page 10, Lines 31-33: I would be more believing of this argument (the kappa values in Gordon et al., 2018, do seem unreasonably high) if you did not find a significant increase in CDNC even with your lower (and probably more realistic) kappa values in this study.

Yes, we didn't see a significant increase in the CDNC due to the BBA. The CDNC increased by BBA is ~13% during July to August in the SEA on average, and only 1.1% in the cloud box region (where most BBA are above the cloud layer). The 56% is only for specific areas.

27. Page 11, Lines 4-6: If you're talking about TOA radiation, isn't the relevant effect that less OLR makes it out due to the radiation coming from the relatively cool cloud tops rather than the warmer surface? Zhou et al. (2017) discuss the potentially important role of LW radiative effects in BBA-cloud interactions.

Yes, we agree. The manuscript has revised as follows:

This may result from the semi-direct enhancement of LWP and cloud cover; therefore, the outgoing longwave radiation at the top of the atmosphere is reduced as it comes from the relatively cool cloud tops rather than the warmer ocean surface, as discussed in Zhou et al. (2017).

28. Page 12, Lines 6-7. Increasing the inversion strength, rather than "lowering the temperature inversion"? Or are you talking about lowering the height of the inversion? I'd argue that has more to do with the clouds not being able to grow via entrainment

We have revised the sentence as below, and changed the "lowering the temperature inversion" to 'strengthening the temperature inversion'.

When BBA accumulate above the inversion, the absorbed shortwave radiation warms the air at the bottom of the inversion layer, strengthening the temperature inversion and decreasing the marine boundary layer height.

29. Page 12, Line 12: Cloud top/base is maybe not the most useful shorthand here, as the increase in SS occurs throughout the cloudy layer near the continent, where the cloud deck is most prevalent in general. The base/top difference only shows up further offshore.

Yes, the cloud base and top differences are over the ocean further offshore; near the continent, CDNC generally increases. We have revised the manuscript as follows:

As a consequence, the BBA absorption effect shows a corresponding response: increasing at low altitudes (cloud bottom in baseline simulation) and decreasing at high altitudes (cloud top from baseline) over the ocean further offshore, and generally increasing near the continent. The microphysical effect decreases the maximum supersaturation, as BBA can act as CCN and allow additional water vapour to condense; however, this decrease is comparatively small. The CDNC over SEA is increased especially further offshore due to the BBA microphysical effect, compensating the decreased CDNC at the higher altitude from the absorption effect. In general, BBA absorption and microphysical effects both contribute to the increase of CDNC, although the former is mainly through affecting the maximum supersaturation while the latter is through increasing CCN.

30. Page 13, Lines 4-5: The global and regional indirect effects are "similar" in that they're both indistinguishable from zero. . . maybe you can argue the global effect is from long range transport and MBL advection, but I wouldn't necessarily highlight this idea in the very last sentence of your paper.

Thanks for the suggestion. We have deleted this sentence.

REVIEWER 2:

This paper uses UKESM1 simulations to study the contribution of different processes to the radiative effects of biomass burning aerosols. The topic is important, the presentation quality is good and the paper shows interesting results. I don't have major concerns about the analysis, but I find there is the need for a more detailed description of the methodology and some additional analysis. I also believe that most of the supplementary figures belong to the main body of the paper (see specific comment below). The paper is worth publishing, but given that it needs additional work in a number of areas, I am recommending a major revision.

Thanks for the positive feedback! Significant reversions have been made to improve the clarity of the manuscript based on the comments from both reviewers.

General comments:

1. Only two years of model simulations are used. They are chosen because they coincide with observational campaigns. However, the observational data are only used to perform an initial assessment of the model's simulations and to justify the use of UKESM1 for the subsequent analysis, which is entirely model-based. Then, why not use a longer simulation period? This will allow to get more robust estimates of the BBA effects in the region, and to quantify the role of interannual variability.

The focus of this manuscript is to investigate the radiative and microphysical effects of BBA in affecting clouds and radiation in the SEA. Those effects are different when BBA are above or below clouds. Therefore, it is critical to simulate the spatial and vertical distribution of the plume. Another crucial task is to have accurate emissions of biomass burning, as it changes interannually. Therefore, we choose to use the GFAS data from satellite measurements to provide the biomass burning emissions. In processing the biomass burning emission data, as we have no information on the vertical distribution of the emission, the emission data was set to emit evenly throughout the boundary layer (representing large fires). However, this method will undoubtedly result in discrepancies of the vertical distribution of BBA. So, we used flight observations to evaluate the model simulation of the BBA. After the evaluation, we confirmed the model did well in simulating the BBA plume in 2016 and 2017, with certain biases regarding the plume distribution. Those evaluations also provide us with the confidence to investigate the BBA effects further, but only for the two evaluated years.

To confirm the biomass burning of the simulated two years is representative, we also calculated the 11 years AOD from the MODIS Terra and Aqua 1-degree product. Then we compared it with the two years AOD from the same MODIS dataset.

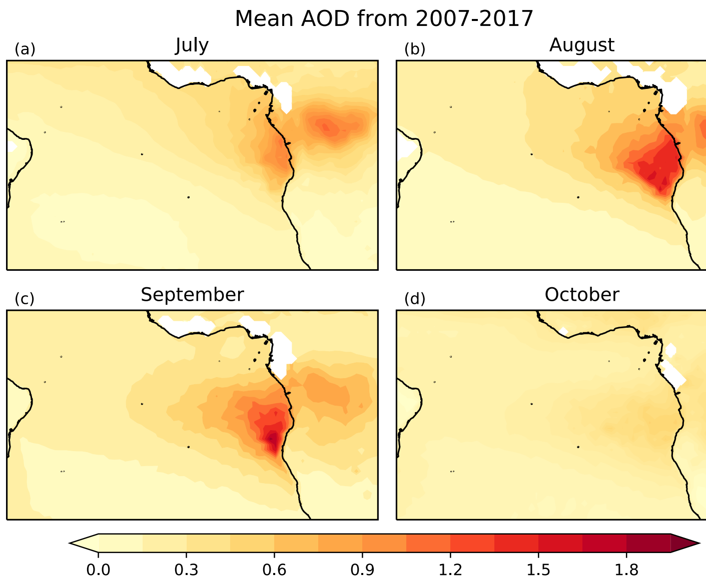

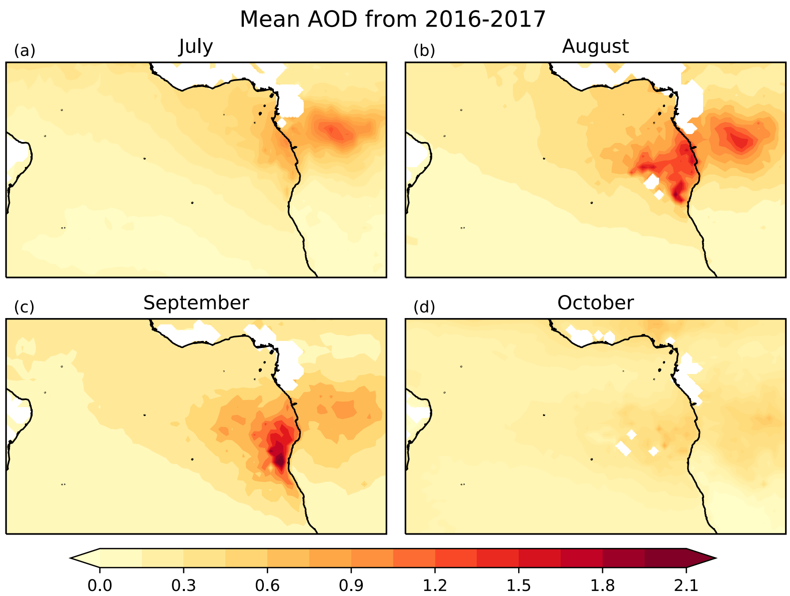

By this comparison, we found that the AOD in the two years average is similar to the climatologies in both magnitude and distribution. Therefore, it is reasonable to use the two years average to represent biomass burning and we leave the analysis of the inter-annual variability to future work.

2. The methodological description needs additional work. Especially, I think a brief description of how the different experiments are combined to decompose the BBA effect into individual contributions is lacking. How accurate is this decomposition? What are the caveats?

We have added more detailed information regarding the decomposition of the BBA effect.

To decompose the BBA effect into radiative and microphysical effects, we performed six simulations from 2016 to 2017, one with present GFAS BBA emission as the baseline simulation ($BB_{0.3}$), and one with the same settings but κ_{org} set to 0 (BB_0); two without BBA emission for κ_{org} set to 0.3 and 0 ($noBB_{0.3}$, $noBB_0$), and two with BBA emissions and κ_{org} set to 0.3 and 0 but with the BBA absorption turned off ($noBB_{0.3}^{noABS}$, $noBB_0^{noABS}$) (setting the imaginary part of the refractive index to zero). Radiative and microphysical effects of BBA are separated using the method of Lu et al., (2018), and described by following equations:

Absorption effect = $BB_0 - BB_0^{noABS}$

Scattering effect = $BB_0^{noABS} - noBB_0$

Total effect = $BB_{0.3} - noBB_{0.3}$

Microphysical effect = Total effect – Absorption effect – Scattering effect

This method allows us to decompose the effects of BBA, with some limitations due to inherent assumptions and model structures. For example, our model only allows us to switch off the absorption of BBA, not the total radiative effects. This assumes that the cloud adjustment due to BBA scattering is negligible in our experiments (which excludes fast adjustments to corresponding surface flux changes). Also note that the microphysical effect of BBA decomposed from our setting is driven by the variation of κ_{org}, thus the small fraction (around 10%) of OC from non-biomass burning emission in this region (figure S1) would contribute a small error.

3. Given that this is a model-based study, the accuracy of the results will not only depend on the representation of the BBA plume and the cloud climatology, but also on how good the model is at representing the cloud response to the drivers of changes. For example, the realism of the strong radiative cooling of the semi-direct effect will depend on how well UKESM1 represents the cloud response to a strengthening of the inversion. Figure S4 touches on this, but only in passing. You cite a reference (Adebiyi et al., 2015) that uses radiosondes to look into this. How does the change in the inversion strength in UKESM1 compare to the one observed with radiosondes? I acknowledge that a comprehensive assessment of how well UKESM1 performs in this respect is out of the scope of this paper, but putting the UKESM1 changes into context would be very helpful.

We have preformed the comparison of radiosonde data and model results, and illustrated in the figure A1. The radiosonde data comes from the paper by Adebiyi et al. (2015). Note that the period of the radiosonde soundings is different, as it was averaged in September and November, from 2000 to 2011; while the model is the September mean from 2016 to 2017. Although the averaged biomass burning condition of those two years are similar to the climatologies, the mean meteorological condition may differ, resulting in changes of the temperature profiles. Another major difference is that the model results are averaged over the whole month, decomposing the effect of absorption explicitly, while the radiosonde was averaged by bins of fine-mode aerosol optical depth (AOD_f). This means that the different radiosonde bins are also likely to correspond to different meteorological situations. As a result, the changes in the radiosonde profiles are more obvious than the model averages, as illustrated in the figure.

The key difference from the figure1 is the change of the mid-tropospheric temperature profile. Stabilisation in the radiosondes also seems to suppress vertical cloud development, which we do not see in the model. Despite those differences, the temperature responses to the BBA are analogous to the measurement; thus, the inversion and cloud response from the model is reasonable. However, how accurate the model can simulate the temperature responses requires additional working to evaluate the model with detailed observation data, and is out of the scope of this manuscript.

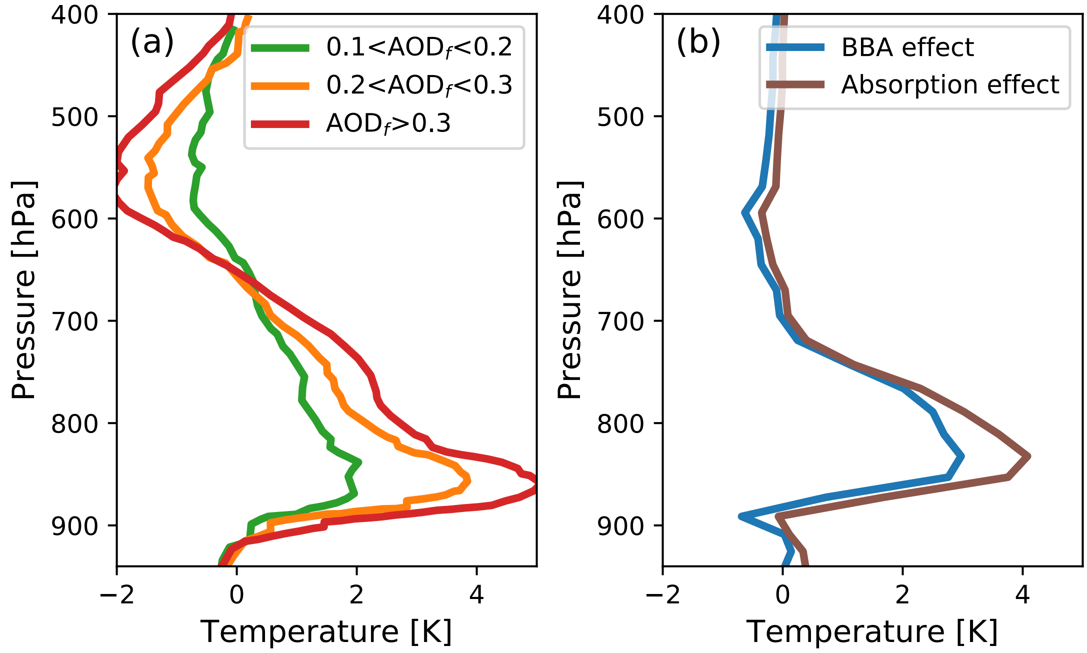

Figure A1. Mean temperature difference profiles in St. Helena Island, calculated from (a) radiosondes (b) UKESM1 model simulation. The differences are constructed by subtracting the mean profiles representing the clean condition, corresponding to (a)$AOD_f < 0.1$ and (b) no BBA simulations. AOD_f is the fine-mode aerosol optical depth, derived from MODIS product. The blue line in (b) is the difference of the temperature profile between simulations with and without BBA, and the brown line is the difference between simulations with absorption on and off. The radiosonde data is from Adebiyi et al. (2015).

The title should be more specific, and should capture the main message of the paper.

Agree. Both reviewers have suggested to make the title more specific. According to the comments, the title has now changed to:

Cloud adjustments dominate the overall negative aerosol radiative effects of biomass burning aerosols in UKESM1 climate model simulations over the south-eastern Atlantic

Specific comments:

1. P3L22-P4L5: Most of this paragraph probably belongs to the methods section. Only the last sentence describes the objectives of the paper. I'd suggest transferring the description of the campaigns to the methods, and expand on what the paper is about.

Thanks for the suggestion, we have made the corresponding revision and moved the description about CLARIFY and ORACLES campaigns into the method section. The last paragraph of the introduction is now revised as below.

The complex interactions between cloud microphysics, radiation, cloud entrainment processes and in particular the small spatial scales involved make the simulation of the stratocumulus clouds deck in the SEA a challenge. Hence, related process studies mainly rely on high-resolution limited-area models (Gordon et al., 2018; Lu et al., 2018) as well as idealized large-eddy simulations (Yamaguchi et al., 2015; Zhou et al., 2017). However, ultimately it is important to represent and constrain the related effects in General Circulation Models (GCM) widely used to investigate climate responses to anthropogenic perturbations, e.g. by the Intergovernmental Panel on Climate Change (IPCC). In this paper, we use the UK Earth System Model (UKESM1), which is also being used in the recent Coupled Model Intercomparison Project Phase 6, to study the BBA effect on the clouds and radiation in the SEA. A detailed description of the model, simulation setup and the data we used for evaluation is provided in section 3. The model is evaluated by observations in section 3.1, and BBA effects on clouds are investigated by decomposition into radiative effects (absorption and scattering) and microphysical effects in section 3.2. The BBA radiative forcing is studied in section 3.3. Section 4 offers conclusions and discussion.

2. Figure 1. The spatial resolution of the model results seems to be much higher than N96. Am I misinterpreting what that figure shows?

Figure 1 shows the measured and collocated model extinction. For each point of the measurement, the model was interpolated to the same point (same coordinate), as described in the method section. By doing this collocation, the model gives point to point data to compare with the measurement; therefore, it's not on the N96 resolution.

3. Figure 3 caption. "The domain in Fig. 3a, ranging from 30◦ S to 10◦ N and from 40◦ W to 30◦ E, is the areas this paper interested in." I believe the description of the area of interest belongs to the main text.

Thanks for the suggestion. We have now added the description of the area into the main text.

BBA can serve as CCN and further impact the CDNC and cloud optical depth. Meanwhile, it also has a significant impact on the atmospheric thermal structure and therefore, the maximum cloud supersaturation, LWP and cloud albedo. The BBA effects on clouds are decomposed as radiative (absorption and scattering) and microphysical effects (detailed in section 2), and their impact on the clouds is examined in this section. Figure 3 provides the baseline cloud properties from the standard simulation. The domain in Fig. 3a, ranging from 30° S to 10° N and from 40° W to 30° E, is the areas this paper interested in. To get BBA effects on the stratocumulus clouds, a cloud box area is used to represent the stratocumulus cloud deck region (the grey box in Fig. 3a). The mean low cloud fraction is 0.58 in the cloud box region, and its western border reaches the area where stratocumulus to cumulus transition occurs (See Fig. 1 in Gordon et al. (2018)), suggesting the dominant of the stratocumulus clouds in this area.

4. Figure 3 caption. " The grey box in the map (cloud box) representing the cloud areas where the averaged low cloud fraction is above 0.58." That would be the 0.58 isoline, unlikely to have a rectangular shape. Please provide a clearer explanation of what this box is.

This cloud box is selected to represent the area where the cumulus and stratocumulus dominate. By using this cloud box, we can assess the BBA effects on the clouds more specifically. Klein and Hartmann (1993) used a similar method to define the stratocumulus clouds region, while our cloud box region is broader, as we want to encompass stratocumulus and some cumulus clouds. As discussed in Gordon et al. (2018), Ascension Island and nearby is within the area where the stratocumulus to cumulus transition occurs. Therefore, we included Ascension Island inside the west boundary of our cloud box region. The mean cloud fraction of this region is 0.58, which confirms the dominant influence of clouds in this region.

5. P7L18. supersaturation (SS). This is an unfortunate acronym. In general, I don't see the need for using an acronym to compress a single word. For instance, we don't normally use MP for microphysics. Or, what would you use for subsaturation?

Though the acronym of supersaturation is widely used in the field measurements and laboratory studies (Meng et al. (2014), Jung et al. (2018), Zhang et al. (2012), Panicker et al. (2020) and Bhattu and Tripathi (2015)), to avoid unnecessary misunderstanding, we have adopted the reviewer's suggestion, and changed it to supersaturation in the manuscript.

6. P9L2. "LWP from BBA absorption shows a steady negative gradient from west to east". I might be looking at the wrong region, but the gradient in the cloud region looks positive to me. Please clarify.

We changed this sentence as below:

The increased LWP from BBA absorption is mainly located near the continent where the BBA and clouds are well separated, indicating the role of BBA in modulating the cloud distribution.

7. Figure 7. This figure shows changes in cloud albedo using the ISCCP simulator. I might have missed it, but I believe that the use of the ISCCP simulator is not documented in the methodology. Which simulator variables are used? Why is this approach better than looking at changes in cloud fraction and cloud radiative effect?

The object of this manuscript is to study different BBA effects on clouds. The changes of cloud fraction are very similar to the changes of LWP, please see the figure below.

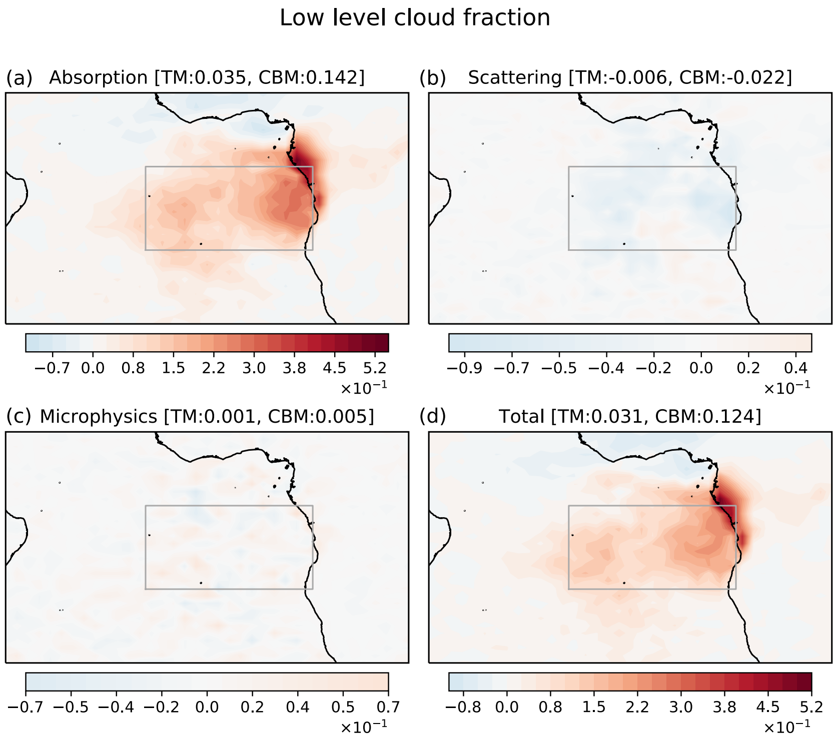

The pattern of the cloud albedo, however, shows a different pattern, as the increased cloud albedo from the absorption effect is in a relatively small area and not so strong. Therefore, we choose to discuss the changes in cloud albedo. Another reason is that cloud albedo is widely used in satellite studies (e.g., Deaconu et al. (2019)); it is an important parameter to assess the cloud radiation properties. Thus, put the cloud albedo in the manuscript allow to compare with satellite studies and understand the role of different BBA properties in affecting the cloud albedo.

Cloud albedo in the UKESM1 is diagnosed by the ISCCP simulator, which is a part of the Cloud Feedback Model Intercomparison Project (CFMIP) Observational Simulator Package (COSP). An additional benefit of using ISCCP output is that it also facilitates model intercomparison by minimizing the impacts of how clouds are defined in different parameterizations. More detailed information and evaluation of the ISCCP are provided by Mace et al. (2011).

In the manuscript, we have now added a brief description of the ISCCP simulator in the context, as below.

In the UKESM1, cloud albedo is diagnosed by the International Satellite Cloud Climatology Project (ISCCP) simulator (Bodas-Salcedo et al., 2011), which can minimize the impacts of how clouds are defined in different parameterizations and facilitate model intercomparison.

8. Discussion of Figure 8c. It would be nice to show a plot with the actual change in the strength of the inversion that drives this strong semi-direct effect.

Thanks for the suggestion. Both reviewers have raised this, and we have added the changes in the temperature profile in the supplement as Fig. S5.

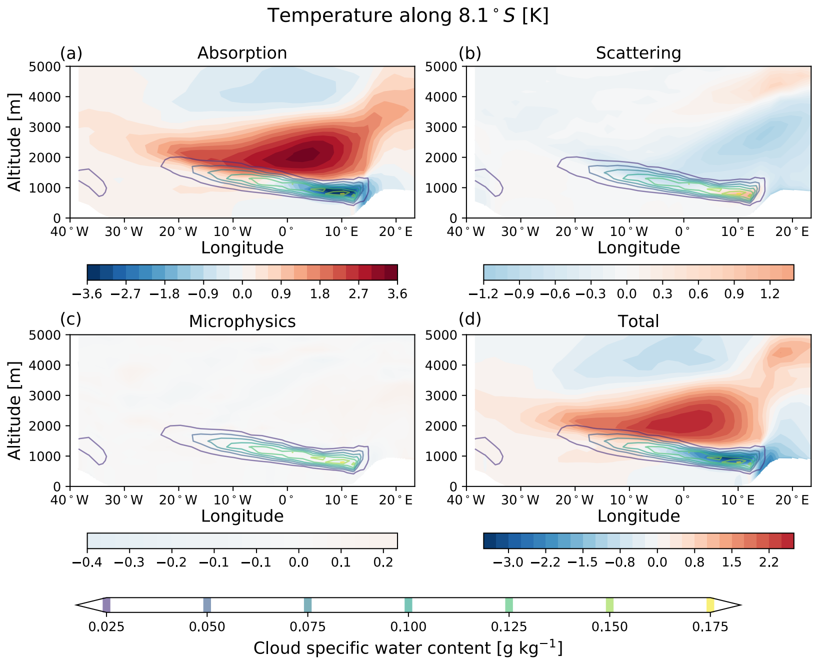

Figure S5. UKESM1 simulated mean vertical profiles of the BBA effects (a) absorption, (b) scattering, (c) microphysical and (d) total on temperature along the latitude of Ascension Island (cf. Fig. 3a) during July and August, 2016-2017. The contour lines are the baseline cloud specific water content. The same colourmap scale is used in each plot to facilitate comparison, but the colourmap ranges differ in each plot, corresponding to the maximum and minimum of temperature at each.

9. Figures S5 to S8. I feel that these figures belong to the main paper, not to the supplementary material. They can be arranged all together in a multi-panel figure with showing the baseline climatologies, complementing the figures showing the changes due to different processes.

Thanks for the suggestion! We have now combined those figures and put them into the main part of the paper.

3.2 Biomass burning aerosol impacts on clouds

BBA can serve as CCN and further impact the CDNC and cloud optical depth. Meanwhile, it also has a significant impact on the atmospheric thermal structure and therefore, the maximum cloud supersaturation, cloud droplets and cloud albedo. The BBA effects on clouds are decomposed into radiative (absorption and scattering) and microphysical effects (detailed in section 2), and their impact on the clouds is examined in this section. Figure 3 provides the baseline cloud properties from the standard simulation. The domain in Fig. 3a, ranging from 30° S to 10° N and from 40° W to 30° E, is the areas this paper interested in. To get BBA effects on the stratocumulus clouds, a cloud box area is used to represent the stratocumulus cloud deck region (the grey box in Fig. 3a). The mean low cloud fraction is 0.58 in the cloud box region, and its western border reaches the area where stratocumulus to cumulus transition occurs (See figure 1 in Gordon et al. (2018)), suggesting the dominance of stratocumulus clouds in this area.

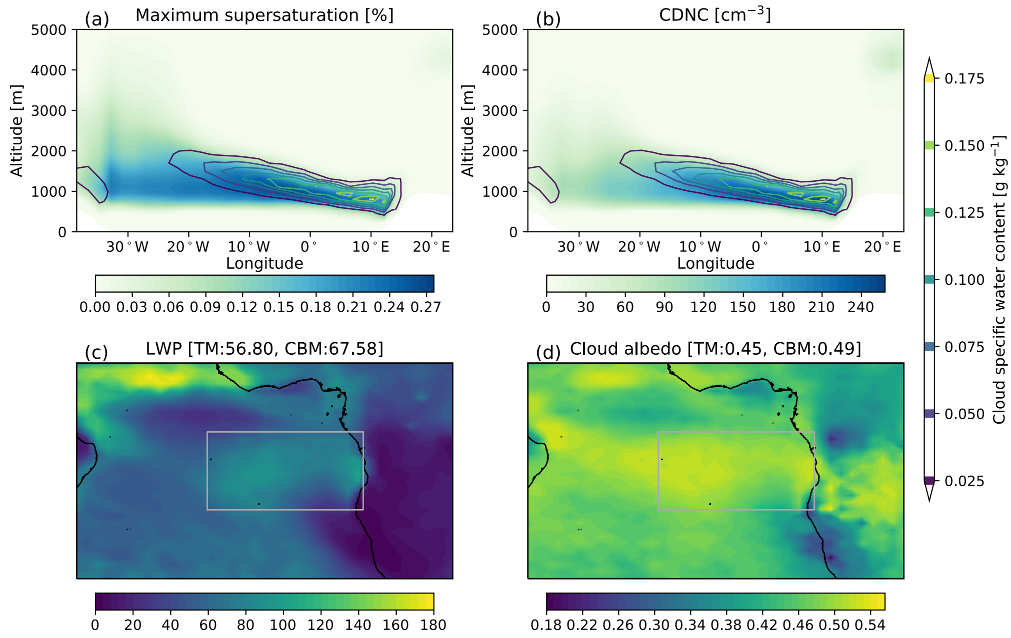

Figure 3. UKESM1 simulated mean (a) vertical profiles of maximum supersaturation and (b) vertical profiles of cloud droplet number concentration along the latitude of Ascension Island; spatial distribution of (c) cloud liquid water path and (d) cloud albedo from the International Satellite Cloud Climatology Project (ISCCP) simulator. These means are averaged during July and August, 2016-2017. The contour lines in (a-b) are the cloud specific water content. The TM in (c-d) is the total mean of the domain, and the CBM is the mean of the cloud box (the grey box on the map) representing areas where the average low cloud fraction is above 0.58.

References:

Adebiyi, A. A. and Zuidema, P.: The role of the southern African easterly jet in modifying the southeast Atlantic aerosol and cloud environments, Quarterly Journal of the Royal Meteorological Society, 142(697), 1574–1589, doi:10.1002/qj.2765, 2016.

Adebiyi, A. A., Zuidema, P. and Abel, S. J.: The Convolution of Dynamics and Moisture with the Presence of Shortwave Absorbing Aerosols over the Southeast Atlantic, J. Climate, 28(5), 1997–2024, doi:10.1175/JCLI-D-14-00352.1, 2015.

Bhattu, D. and Tripathi, S. N.: CCN closure study: Effects of aerosol chemical composition and mixing state, Journal of Geophysical Research: Atmospheres, 120(2), 766–783, doi:10.1002/2014JD021978, 2015.

Bodas-Salcedo, A., Webb, M. J., Bony, S., Chepfer, H., Dufresne, J.-L., Klein, S. A., Zhang, Y., Marchand, R., Haynes, J. M., Pincus, R. and John, V. O.: COSP: Satellite simulation software for model assessment, Bull. Amer. Meteor. Soc., 92(8), 1023–1043, doi:10.1175/2011BAMS2856.1, 2011.

Chand, D., Wood, R., Anderson, T. L., Satheesh, S. K. and Charlson, R. J.: Satellite-derived direct radiative effect of aerosols dependent on cloud cover, Nature Geoscience, 2(3), 181–184, doi:10.1038/ngeo437, 2009.

Deaconu, L. T., Ferlay, N., Waquet, F., Peers, F., Thieuleux, F. and Goloub, P.: Satellite inference of water vapor and aerosol-above-cloud combined effect on radiative budget and cloud top processes in the Southeast Atlantic Ocean, Atmospheric Chemistry and Physics Discussions, 1–34, doi:https://doi.org/10.5194/acp-2019-189, 2019.

Diamond, M. S., Dobracki, A., Freitag, S., Small Griswold, J. D., Heikkila, A., Howell, S. G., Kacarab, M. E., Podolske, J. R., Saide, P. E. and Wood, R.: Time-dependent entrainment of smoke presents an observational challenge for assessing aerosol–cloud interactions over the southeast Atlantic Ocean, Atmospheric Chemistry and Physics, 18(19), 14623–14636, doi:https://doi.org/10.5194/acp-18-14623-2018, 2018.

Gordon, H., Field, P. R., Abel, S. J., Dalvi, M., Grosvenor, D. P., Hill, A. A., Johnson, B. T., Miltenberger, A. K., Yoshioka, M. and Carslaw, K. S.: Large simulated radiative effects of smoke in the south-east Atlantic, Atmospheric Chemistry and Physics, 18(20), 15261–15289, doi:https://doi.org/10.5194/acp-18-15261-2018, 2018.

Gupta, P., Remer, L. A., Patadia, F., Levy, R. C. and Christopher, S. A.: High-Resolution Gridded Level 3 Aerosol Optical Depth Data from MODIS, Remote Sensing, 12(17), 2847, doi:10.3390/rs12172847, 2020.

Herbert, R. J., Bellouin, N., Highwood, E. J. and Hill, A. A.: Diurnal cycle of the semi-direct effect from a persistent absorbing aerosol layer over marine stratocumulus in large-eddy simulations, Atmospheric Chemistry and Physics, 20(3), 1317–1340, doi:https://doi.org/10.5194/acp-20-1317-2020, 2020.

Jung, C. H., Yoon, Y. J., Kang, H. J., Gim, Y., Lee, B. Y., Ström, J., Krejci, R. and Tunved, P.: The seasonal characteristics of cloud condensation nuclei (CCN) in the arctic lower troposphere, Tellus B: Chemical and Physical Meteorology, 70(1), 1–13, doi:10.1080/16000889.2018.1513291, 2018.

Kacarab, M., Thornhill, K. L., Dobracki, A., Howell, S. G., O’Brien, J. R., Freitag, S., Poellot, M. R., Wood, R., Zuidema, P., Redemann, J. and Nenes, A.: Biomass burning aerosol as a modulator of the droplet number in the southeast Atlantic region, Atmospheric Chemistry and Physics, 20(5), 3029–3040, doi:https://doi.org/10.5194/acp-20-3029-2020, 2020.

Klein, S. A. and Hartmann, D. L.: The Seasonal Cycle of Low Stratiform Clouds, J. Climate, 6(8), 1587–1606, doi:10.1175/1520-0442(1993)006<1587:TSCOLS>2.0.CO;2, 1993.

Lu, Z., Liu, X., Zhang, Z., Zhao, C., Meyer, K., Rajapakshe, C., Wu, C., Yang, Z. and Penner, J. E.: Biomass smoke from southern Africa can significantly enhance the brightness of stratocumulus over the southeastern Atlantic Ocean, PNAS, 115(12), 2924–2929, doi:10.1073/pnas.1713703115, 2018.

Mace, G. G., Houser, S., Benson, S., Klein, S. A. and Min, Q.: Critical Evaluation of the ISCCP Simulator Using Ground-Based Remote Sensing Data, J. Climate, 24(6), 1598–1612, doi:10.1175/2010JCLI3517.1, 2011.

Meng, J. W., Yeung, M. C., Li, Y. J., Lee, B. Y. L. and Chan, C. K.: Size-resolved cloud condensation nuclei (CCN) activity and closure analysis at the HKUST Supersite in Hong Kong, Atmospheric Chemistry and Physics, 14(18), 10267–10282, doi:https://doi.org/10.5194/acp-14-10267-2014, 2014.

Mulcahy, J. P., Johnson, C., Jones, C. G., Povey, A. C., Scott, C. E., Sellar, A., Turnock, S. T., Woodhouse, M. T., Abraham, N. L., Andrews, M. B., Bellouin, N., Browse, J., Carslaw, K. S., Dalvi, M., Folberth, G. A., Glover, M., Grosvenor, D., Hardacre, C., Hill, R., Johnson, B., Jones, A., Kipling, Z., Mann, G., Mollard, J., O’Connor, F. M., Palmieri, J., Reddington, C., Rumbold, S. T., Richardson, M., Schutgens, N. A. J., Stier, P., Stringer, M., Tang, Y., Walton, J., Woodward, S. and Yool, A.: Description and evaluation of aerosol in UKESM1 and HadGEM3-GC3.1 CMIP6 historical simulations, Geoscientific Model Development Discussions, 1–59, doi:https://doi.org/10.5194/gmd-2019-357, 2020.

O’Connor, F. M., Johnson, C. E., Morgenstern, O., Abraham, N. L., Braesicke, P., Dalvi, M., Folberth, G. A., Sanderson, M. G., Telford, P. J., Voulgarakis, A., Young, P. J., Zeng, G., Collins, W. J. and Pyle, J. A.: Evaluation of the new UKCA climate-composition model – Part 2: The Troposphere, Geosci. Model Dev., 7(1), 41–91, doi:10.5194/gmd-7-41-2014, 2014.

Panicker, A. S., Anil Kumar, V., Raju, M. P., Pandithurai, G., Safai, P. D., Beig, G. and Das, S.: CCN activation of carbonaceous aerosols from different combustion emissions sources: A laboratory study, Atmospheric Research, 248, 105252, doi:10.1016/j.atmosres.2020.105252, 2020.

Schutgens, N. A. J., Gryspeerdt, E., Weigum, N., Tsyro, S., Goto, D., Schulz, M. and Stier, P.: Will a perfect model agree with perfect observations? The impact of spatial sampling, Atmos. Chem. Phys., 16(10), 6335–6353, doi:10.5194/acp-16-6335-2016, 2016.

Woodward, S.: Modeling the atmospheric life cycle and radiative impact of mineral dust in the Hadley Centre climate model, Journal of Geophysical Research: Atmospheres, 106(D16), 18155–18166, doi:10.1029/2000JD900795, 2001.

Yamaguchi, T., Feingold, G., Kazil, J. and McComiskey, A.: Stratocumulus to cumulus transition in the presence of elevated smoke layers, Geophysical Research Letters, 42(23), 10,478-10,485, doi:10.1002/2015GL066544, 2015.

Zhang, Q., Meng, J., Quan, J., Gao, Y., Zhao, D., Chen, P. and He, H.: Impact of aerosol composition on cloud condensation nuclei activity, Atmospheric Chemistry and Physics, 12(8), 3783–3790, doi:10.5194/acp-12-3783-2012, 2012.

Zhou, X., Ackerman, A. S., Fridlind, A. M., Wood, R. and Kollias, P.: Impacts of solar-absorbing aerosol layers on the transition of stratocumulus to trade cumulus clouds, Atmospheric Chemistry and Physics, 17(20), 12725–12742, doi:https://doi.org/10.5194/acp-17-12725-2017, 2017.

Zuidema, P., Sedlacek, A. J., Flynn, C., Springston, S., Delgadillo, R., Zhang, J., Aiken, A. C., Koontz, A. and Muradyan, P.: The Ascension Island Boundary Layer in the Remote Southeast Atlantic is Often Smoky, Geophysical Research Letters, 45(9), 4456–4465, doi:10.1002/2017GL076926, 2018.

Revised manuscript

Cloud adjustments dominate the overall negative aerosol radiative effects of biomass burning aerosols in UKESM1 climate model simulations over the south-eastern Atlantic ~~The significant role of biomass burning aerosols in clouds and radiation in the South-eastern Atlantic Ocean~~

Haochi Che[1, a], Philip Stier[1], Hamish Gordon[2, b], Duncan Watson-Parris[1], Lucia Deaconu[1]

[1]Atmospheric, Oceanic and Planetary Physics, Department of Physics, University of Oxford, Oxford, OX1 3PU, UK
[2]School of Earth and Environment, University of Leeds, LS2 9JT, UK
[a]now at: Department of Geophysics, Tel-Aviv University, 69978, Israel
[b]now at: Engineering Research Accelerator, Carnegie Mellon University, Pittsburgh, PA 15217, United States

Correspondence to: Haochi Che (haochiche@tauex.tau.ac.il)

Abstract

The South-eastern Atlantic Ocean (SEA) is semi-permanently covered by one of the most extensive stratocumulus cloud decks on the planet and experiences about one-third of the global biomass burning emissions from the southern Africa savannah region during the fire season. To get a better understanding of the impact of these biomass burning aerosols on clouds and radiation balance over the SEA, the latest generation of the UK Earth System Model (UKESM1) is employed. Measurements from the CLARIFY and ORACLES flight campaigns are used to evaluate the model, demonstrating that the model has good skill in reproducing the biomass burning plume. To investigate the underlying mechanisms in detail, the effects of biomass burning aerosols on the clouds are decomposed into radiative effects (via absorption and scattering) and microphysical effects (via perturbation of cloud condensation nuclei (CCN) and cloud microphysical processes). The July-August means are used to characterise aerosols, clouds and the radiation balance during the fire season. Results show around ~~68~~65% of CCN at 0.2% supersaturation in the SEA domain can be attributed to biomass burning. The absorption effect of biomass burning aerosols is the most significant in affecting clouds and radiation. Near the continent, it increases the maximum supersaturation diagnosed by the activation scheme, while further from the continent it reduces the altitude of the maximum supersaturation. As a result, the cloud droplet number concentration responds with ~~shows~~ a similar pattern to the absorption effect of biomass burning aerosols. The microphysical effect, however, ~~of biomass burning aerosols~~ decreases the maximum supersaturation and increases the cloud droplets concentration over the ocean; ~~however,~~although this change is relatively small. The liquid water path is also significantly increased over the SEA (mainly caused by the absorption effect of biomass burning aerosols) when biomass burning aerosols are above the stratocumulus cloud deck. The microphysical pathways lead to a slight increase in the liquid water path over the ocean. These changes in cloud properties indicate the significant role of biomass burning aerosols

on clouds in this region. Among the effects of biomass burning aerosols on the radiation balance, the semi-direct radiative effects (rapid adjustments induced by biomass burning aerosols radiative effects) have a dominant cooling impact over the SEA, which offset the warming direct radiative effect (radiative forcing from biomass burning aerosol–radiation interactions) and lead to overall net cooling radiative effect in the SEA. However, the magnitude and the sign of the semi-direct effects are sensitive to the relative location of biomass burning aerosols and clouds, reflecting the critical task of the accurate modelling of the biomass burning plume and clouds in this region.~~.~~ ~~However, the magnitude and the sign of the semi-direct effects are dependent on the relative location of biomass burning aerosols and clouds. The net biomass burning aerosols radiative effect shows a negative cooling effect in the SEA, indicating the significant role of biomass burning aerosols in affecting the regional radiation balance and climate.~~

1 Introduction

The South-eastern Atlantic Ocean (SEA) is covered semi-permanently by one of the most extensive stratocumulus cloud decks on the planet (Wood, 2012). These clouds reflect a significant amount of solar radiation. Hence, even a moderate change in the cloud deck coverage (15-20 % increase) or liquid water path (20-30 % increase) would produce a negative radiative effect that could completely compensate the radiative forcing of greenhouse gases (Wood, 2012). From July through October, the widespread biomass burning across the savannah region in southern Africa contributes about one-third of the global biomass burning emissions (Roberts et al., 2009; van der Werf et al., 2010). The emitted biomass burning aerosols (BBA) in southern Africa are transported over the SEA, resulting in different impacts on the underlying stratocumulus deck and radiative balance through multiple interactions (Adebiyi and Zuidema, 2016; Wilcox, 2012; Wood, 2012).

BBA can warm the lower troposphere and modify the radiation budget as they absorb shortwave radiation. At the top of atmosphere, BBA can exert either a cooling or a warming shortwave direct radiative effect (radiative forcing from BBA–radiation interactions) depending on the underlying layer brightness (e.g., ocean or stratocumulus cloud deck) (Chand et al., 2009; Wilcox, 2012). Despite the fact that intensive studies have been performed (Chand et al., 2009; Lu et al., 2018; Sakaeda et al., 2011; Stier et al., 2013; Wilcox, 2012), there is still no consensus on the magnitude or even the sign of the BBA direct radiative effect over the SEA. This discrepancy is primarily owing to the uncertainties in the underlying cloud coverage (Stier et al., 2013) and the BBA spatial distribution; therefore, accurate modelling of the spatial and vertical distribution of the BBA plume and clouds is a critical task in this area.

The interactions between BBA and the underlying cloud deck adds additional complication as BBA can alter the thermodynamic structure of the atmosphere (through rapid adjustments induced by BBA radiative effects, i.e., semi-direct effects) and also serve as additional cloud condensation nuclei (CCN). The former is referred to as BBA radiative effect on cloud, and the latter is BBA microphysical effect on cloud. Both effects have a significant impact on the cloud liquid water path (LWP), cloud coverage, and radiation balance (Gordon et al., 2018; Lu et al., 2018; Wilcox, 2010). When the BBA layer is above the cloud deck, its radiative effect can enhance the existing temperature inversion and therefore stability, inhibiting cloud-top entrainment. As a consequence, boundary layer relative humidity is preserved and cloud coverage maintained. This could lead to an increase of LWP, optically thicker clouds, and therefore an additional cooling semi-direct effect - potentially of comparable magnitude to the warming BBA direct radiative effect, resulting in both the sign and the magnitude of the total BBA radiative effect remaining unclear (Deaconu et al., 2019; Sakaeda et al., 2011; Wilcox, 2010, 2012). Previous efforts mainly focused on the above cloud BBA radiative effect, as the BBA plume is generally well separated from the underlying cloud deck in their experiments (Hobbs, 2002; Wilcox, 2012). However, recent studies found abundant biomass burning influence within the marine boundary layer (MBL) at Ascension Island from in-situ observations (Zuidema et al., 2018) and throughout the SEA from flight measurements (Diamond et al., 2018; Kacarab et al., 2020), confirming the interaction of BBA and clouds~~However, recent studies found that parts of the plume enters the marine boundary layer (MBL) and interacts with clouds (LeBlanc et al., 2019; Lu et al., 2018)~~. These findings are also supported by the possible BBA effects on changing cloud properties from satellite observations (Costantino and Bréon, 2010, 2013; Painemal et al., 2014).~~ Moreover, studies have suggested that as the MBL deepens further offshore, most BBA subsides and are entrained into the MBL (Costantino and Bréon, 2010, 2013; Gordon et al., 2018; Painemal et al., 2014).~~ When the BBA plume enters and interacts with clouds, the microphysical effect of BBA is non-negligible, as BBA can serve as CCN, become activated, and increase the CDNC, resulting in optically thicker clouds of higher albedo (Twomey, 1974, 1977). However, some studies have found that when the LWP remains constant, the increased CDNC will increase cloud-top entrainment by the fast evaporation of small droplets at the cloud top, which, in return, can reduce cloud fraction and LWP (Wood, 2012). As a result, the BBA microphysical effect on clouds may be diminished or even cancelled out under some scenarios (Ackerman et al., 2004; Wood, 2007). A recent study found the BBA number concentration and hygroscopicity played different roles in modulating CDNC concentration in clean and polluted environments (Kacarab et al., 2020), ad~~d~~ding more uncertainty of the BBA microphysical effect. As to the BBA radiative effects, when BBA enter the clouds, it can *"burn off"* clouds by absorbing shortwave solar radiation, warming the air and the accompanying increase in saturation vapour pressure (Hansen et al., 1997; Hill et al., 2008; Koch and Genio, 2010), which can lead to a decrease of both the cloud LWP and the cloud coverage. Therefore, BBA microphysical and radiative effects can play an opposing role for cloud physical and radiative properties, creating significant uncertainties in the net effective radiative forcing (change in net downward radiative flux at the top of the atmosphere after allowing rapid adjustments) associated with BBA in the SEA area. Hence, it is critical to assess the BBA effects over the SEA during the fire season using a model that can account for all the relevant processes.

The complex interactions between cloud microphysics, radiation, cloud entrainment processes and in particular, the small spatial scales involved make the simulation of the stratocumulus clouds deck in the SEA a challenge. Hence, related process studies mainly rely on high-resolution limited-area models (Gordon et al., 2018; Lu et al., 2018) as well as idealized large-eddy simulations (Yamaguchi et al., 2015; Zhou et al., 2017). However, ultimately it is important to represent and constrain the related effects in General Circulation Models (GCM) widely used to investigate climate responses to anthropogenic perturbations, e.g. by the Intergovernmental Panel on Climate Change (IPCC). ~~Furthermore, to have a better understanding of the simulation and errors of the stratocumulus cloud deck and BBA layer over the SEA in current climate models, the GCM is a necessary tool.~~ In this paper, we use the UK Earth System Model (UKESM1), which is also being used in the recent Coupled Model Intercomparison Project Phase 6, to study the BBA effects on the clouds and radiation in the SEA. A detailed description of the model, simulation setup and the data we used for evaluation is in section 2. The model is evaluated by observations in section 3.1, and BBA effects on clouds are investigated by decomposition into radiative effects (absorption and scattering) and microphysical effects in section 3.2. The BBA radiative forcing is studied in section 3.3. Section 4 offers conclusions and discussion.

~~To evaluate the model performance, we use two flight campaigns that took place in the SEA to compare with the model simulation. One is the ORACLES (Observations of Aerosols above Clouds and their interactions) campaign (Redemann et al., in preparation) including three deployments, which were conducted from Namibia in 2016 and from São Tomé in 2017, 2018 (not used), ranging from the west coast of Africa to Ascension Island. The other is the CLARIFY (Clouds and Aerosol Radiative Impacts and Forcing: Year 2016) campaign (Haywood et al., in preparation), which was conducted from Ascension Island in 2017, and located around the Ascension Island. These flight campaigns were carried out during the biomass burning seasons, and are able to provide an ideal dataset covering both BBA above and interacting with clouds, as previous studies have found that the BBA plume layer generally subsides and meets the gradually deepening marine boundary layer in the vicinity of Ascension Island and St Helena (Adebiyi et al., 2015)(Diamond et al., 2018). In this paper, we combine simulations using the UK Earth System Model (UKESM1) with CLARIFY and ORACLES aircraft campaigns to decompose the effect of the BBA plume into radiative effects and the microphysical effects, and ultimately investigate the effective radiative forcing associated with aerosol-cloud interactions in the SEA.~~

2 Method

The first version of the United Kingdom Earth System Model, UKESM1(Sellar et al., 2019) is the latest Earth system model developed jointly by the UK's Met Office and Natural Environment Research Council (NERC). The core of UKESM1 is based on the Hadley Centre Global Environmental Model version 3 (HadGEM3) Global Coupled (GC) climate configuration of the Unified Model (UM) (Hewitt et al., 2011), comprised of the UM atmosphere (Walters et al., 2017), ocean (Storkey et al., 2018), land surface and sea ice components (Ridley et al., 2018; Walters et al., 2017). Aerosol and its interaction with clouds are represented by the UK Chemistry and Aerosol model (UKCA) (Mulcahy et al., 2020; O'Connor et al., 2014), including the modal aerosol microphysics ~~scheme~~ GLOMAP (Mann et al., 2010), with five interactive log-normal aerosol modes (four soluble modes from nucleation to coarse, and one insoluble of Aitken mode) comprised of internally-mixed sulfate, sea salt, black carbon, and organic carbon~~comprised of sulfate, sea salt, black carbon, and organic carbon chemical components~~. Mineral dust is represented separately by an externally mixed bin representation (Woodward, 2001).

For BBA emissions, we use the global fire assimilation system (GFAS) version 1 data. GFAS is based on satellite fire radiative power (FRP) products and has been operating in real-time under Monitoring Atmospheric Composition and Change (MACC) project (Kaiser, J.W. et al., 2012). The GFAS biomass burning emissions are scaled by 2.0 to improve the agreement with observations, as suggested in the model configuration (Johnson et al., 2016), with scale factors commonly used for this emission inventory (Kaiser, J.W. et al., 2012). For other emissions, the Coupled Model Intercomparison Project Phase 6 (CMIP6) emission data during 2014 are used (Eyring et al., 2016; Gidden et al., 2019).

The model is configured as Global Atmosphere 7.1 (GA7.1), and our simulations run with a horizontal resolution of N96, i.e., 1.875º × 1.25º, and 85 vertical levels. The sea surface temperatures and sea ice are prescribed with daily reanalysis data (Reynolds et al., 2007). The model simulations are nudged every 6 h by ERA-Interim horizontal wind fields above 1500 m (Telford et al., 2008), while the temperature is not nudged to allow the fast adjustments by the BBA, following the recommendations of Zhang et al., (2014). The kappa-Kohler activation scheme is used in the model, with the kappa value of organic carbon (OC) κ_{org} set to 0.3 (Chang et al., 2010). To decompose the BBA effect into radiative and microphysical effects, we performed six simulations from 2016 to 2017, one with present GFAS BBA emissions as the baseline simulation ($BB_{0.3}$), and one ~~has~~ with the same settings but κ_{org} ~~is~~ set to 0 (BB_0); two without BBA emissions ~~for~~ and κ_{org} set to 0.3 and 0 ($noBB_{0.3}$, $noBB_0$), and two with BBA emissions and ~~for~~ κ_{org} set to 0.3 and 0 but with the BBA absorption turned off ($noBB_{0.3}^{noABS}$, $noBB_{0}^{noABS}$) (setting the imaginary part of the refractive index to zero~~through modification of the refractive indices~~). ~~Then the~~ R~~r~~adiative and microphysical effects of BBA are separated using the method by Lu et al., (2018), and described by following equations~~.~~:

Absorption effect = $BB_0 - BB_0^{noABS}$

Scattering effect = $BB_0^{noABS} - noBB_0$

Total effect = $BB_{0.3} - noBB_{0.3}$

Microphysical effect = Total effect – Absorption effect – Scattering effect

~~as Lu et al., (2018).~~

This method allows us to decompose the effects of BBA, with some limitations due to inherent assumptions and model structures. For example, our model only allows us to switch off the absorption of BBA, not the total radiative effects. This assumes that the cloud adjustment due to BBA scattering is negligible in our experiments (which excludes fast adjustments to corresponding surface flux changes). Also note that the microphysical effect of BBA decomposed from our setting is mainly driven by the variation of κ_{org}, thus the small fraction (around 10%) of OC from non-biomass burning emissions in this region

(Fig. S1) would contribute a small error.~~However, the way to isolate the BBA radiative effect in this paper is slightly different, as our model only allows us to switch off the absorption of BBA. This assumes the cloud adjustment due to BBA scattering is negligible in our experiments. Also note the microphysical effect of BBA decomposed from our setting is driven by the variation of κ_{org}, thus the small fraction (around 10%) of OC from no-biomass burning emission in this region (figure S1) would contribute a small error.~~ Then the BBA radiative effect is further decomposed into direct, indirect (effective radiative forcing from BBA–cloud interactions, defined as rapid adjustments and the net forcing with these adjustments from BBA-cloud interactions), and semi-direct effects by the method of Ghan et al., (2012) and Gordon et al., (2018). Two years are simulated in the model (2016 and 2017), however this analysis focuses on ~~the averages during~~ July and August~~ are used~~, for consistency with the flight campaigns~~, to represent the BBA effects during the African fire season~~. Note although July and August can be used to represent BBA effects during the African fire season (July-October), this selection will also result in some uncertainties, as the BBA distribution and properties change over the course of the fire season, influenced in part by meteorological shifts, such as the strengthening of the southern African Easterly Jet (AEJ-S) in September and October, corresponding to a more elevated plume (Adebiyi and Zuidema, 2016).

To evaluate the model performance, we use two flight campaigns that took place in the SEA to compare with the baseline model simulation. One is the ORACLES (Observations of Aerosols above Clouds and their interactions) campaign (Redemann et al., 2020) including three deployments, which were conducted from Namibia in 2016 and from São Tomé in 2017, 2018 (not used), ranging from the west coast of Africa to Ascension Island. The other is the CLARIFY (Clouds and Aerosol Radiative Impacts and Forcing: Year 2016) campaign (Haywood et al., 2020), which was conducted from Ascension Island in 2017. These flight campaigns were carried out during the biomass burning seasons, and have provided an ideal dataset covering both BBA above and interacting with clouds, as previous studies have found that the BBA plume layer generally subsides and meets the gradually deepening marine boundary layer in the vicinity of Ascension Island and St Helena (Adebiyi et al., 2015). However, observations also indicate that the entrainment of BBA into the MBL can be intermittent, can require significant contact time (Diamond et al., 2018), and that recirculation patterns can result in clean MBL near Ascension Island.

~~To evaluate the model simulated cloud fields and BBA plume over SEA, T~~The aerosol extinction from ORACLES (2016, 2017) and CLARIFY are used to compare with the model data. For ORACLES, we use the dry aerosol scattering and absorption coefficients from TSI nephelometers and Particle Soot Absorption Photometer (PSAP) (Pistone et al., 2019); For CLARIFY, the dry aerosol extinction coefficient was measured by cavity ring down spectroscopy using the EXSCALABAR instrument (Extinction Scattering and Absorption of Light for AirBorne Aerosol Research (Cotterell et al., 2020; Davies et al., 2018)), similar to that reported by Langridge et al. (2011)~~The extinction coefficient measured from Cavity Ring-Down Spectroscopy~~

~~(Langridge et al., 2011) is used for CLARIFY~~. For the comparison, the extinction data from the observations is calculated at 550 nm wavelength, by using its Angström exponent. Then ~~-~~we collocate the three-hourly variables from the baseline model simulation with the aircraft observations (Watson-Parris et al., 2016, 2019). Two different collocation are performed, one to the 4-D coordinates of the observations (time, longitude, latitude, altitude), and another one with 3-D coordinates (time, longitude, latitude), to provide model profiles at the location of the observations. The aerosol optical depth (AOD) at 550 nm from the Moderate Resolution Imaging Spectroradiometer (MODIS) Terra (MOD08_D3, Version 4.4) and Aqua (MYD08_D3, Version 4.4) level 3, 1° × 1° resolution, collection 6 daily products are also used to further evaluate the model performance.

3 Results

3.1 Model evaluation

The spatial and vertical distribution of the BBA plume is critical to the aerosol-cloud interactions, as it can significantly impact the sign and the magnitude of the BBA effects (Bellouin et al., 2019). To evaluate the performance of the model, the spatial and vertical distribution of aerosol extinction coefficient from the model are compared with the aircraft observations

[insert ~~figure~~Fig. 1 here]

The mean spatial distributions of the aerosol extinction coefficient along the flight tracks are illustrated in Fig 1. Note that the modelled extinction is for ambient aerosols, while the measurement gives dry extinction. Although this inter-comparison is widely used in model studies (Shinozuka et al., 2019), it is a potential source of error for model / measurement discrepancies, as the extinction coefficient will generally be larger in the model. From ~~figure~~Fig. 1, the model generally agrees well with the measurements, and it captures the extinction coefficient peak around 2° W; however, it also overestimates the extinction around 5°W. Extinction coefficients are slightly underestimated by the model near the coast of southern Africa and overestimated over the SEA. These errors suggest that the reproduced plume generally agrees well with measurements but is transported too far north and west. These biases might be partly attributable to the coarse model resolution and the use of 3-hourly output, which reduces reliability in the collocation. The comparison of mean July-August ~~September~~ AOD of the model and retrievals (~~at~~ at ambient relative humidity) from the MODIS satellite instrument further confirms this bias (~~Figure~~Fig. S2), which indicates that the model error may be related to the location and initial altitude of biomass burning emissions. Furthermore, the BBA deposition in the model may be biased low.

The mean vertical distribution of the aerosol extinction coefficient is shown in Fig 2. The model extinction coefficient profile is collocated to the 3-D (latitude/longitude/time) coordinate of the observation. It can be seen in the figure that the plume is above clouds from the coast to 2° W, where it shows the extinction peak. From east to west, the plume ~~gradually~~ subsides~~ed~~ and c~~a~~omes into contact with the clouds. At 5° W, the plume is generally inside the clouds, although the actual plume distribution and occurrence of plume-cloud contact at any given time can be more nuanced (Diamond et al., 2018).~~;~~ T~~t~~hus, the

BBA can interact and modulate ~~the~~ cloud properties. This finding is also confirmed by previous studies (Adebiyi et al., 2015; Chand et al., 2009; Deaconu et al., 2019; Gordon et al., 2018). From ~~figure~~Fig. 2, the modelled vertical distribution of BBA plume agrees quite well with the measurements, with the measured peak extinctions generally captured by the model. However, near 11° W, the modelled extinction coefficient has a slightly lower altitude than the measurement. This may indicate that the altitude of the plume is lower in the model, i.e., the model has less aerosol above cloud or aerosol reaches lower when in clear sky, or it may be the result of comparing simulated extinction ~~at~~ at ambient humidity to observations of dry extinction.

[insert ~~figure~~Fig. 2 here]

This comparison shows that the model has skill in reproducing the BBA plume, although the plume is transported slightly too far west and north, and also at a lower altitude towards the western part of the region of interest (westward of 5° W). The bias of the BBA plume location and vertical profile reproduced by the model will contribute to the uncertainty of the BBA microphysical effect over the ocean west of 5° W and of the BBA radiative effect. However, these errors are relatively small as the BBA plume is generally well-simulated in the model, allowing us to investigate the BBA effect on the underlying and interacting cloud and the radiation balance.

3.2 Biomass burning aerosols impacts on clouds

BBA can serve as CCN and further impact the CDNC and cloud optical depth. Meanwhile, it also has a significant impact on the atmospheric thermal structure and therefore~~,~~ the maximum cloud supersaturation~~ (SS)~~, ~~LWP~~ cloud droplet concentration and cloud albedo. The BBA effects on clouds are decomposed ~~as~~ into radiative (absorption and scattering) and microphysical effects (detailed in section 2), and their impact on the clouds is examined in this section. Figure 3 provides the baseline cloud properties from the standard simulation. The domain in Fig. 3a, ranging from 30° S to 10° N and from 40° W to 30° E, is the focus area of this paper. To get BBA effects on the stratocumulus clouds, a cloud box area is used to represent the stratocumulus cloud deck region (the grey box in Fig. 3a). The mean low cloud fraction is 0.58 in the cloud box region, and its western border reaches the area where the stratocumulus to cumulus transition occurs (See Fig. 1 in ~~(~~Gordon et al. (~~,~~2018)), suggesting the dominance of stratocumulus clouds in this area.

[insert Fig. 3 here]

3.2.1 Biomass burning aerosols effects on CCN

[insert ~~figure~~Fig. ~~3~~ 4 here]

CCN from BBA mainly occurs over land and in the eastern part of the SEA. From east to west, a sharp gradient of BBA $CCN_{0.2\%}$ (CCN at 0.2% supersaturation) is evident in Fig ~~3~~4 (a), which may be due to the strong aerosol wet and dry removal mechanisms over the SEA, resulting in only BBA with a very small diameter being transported so far away from the continent. Due to the low hygroscopicity of BBA, the small-diameter particles (below 0.1 μm) are unable to activate. Furthermore, these fine particles decrease the average hygroscopicity of internally mixed aerosols, thus can reduce the CCN concentration. The budget of $CCN_{0.2\%}$ attributed to BBA account for ~ ~~68~~65% of total $CCN_{0.2\%}$ in the cloud box (grey box) and ~ ~~50~~40% in the whole domain (~~Figure~~Fig. S3), indicating that BBA is the dominant source of CCN in the marine stratocumulus deck area.

The BBA $CCN_{0.2\%}$ profile along the latitude of Ascension Island (~~Fig.~~Fig. ~~3b~~4b) shows a distinct gradient. With near-source concentrations of 1000 cm^{-3}, the BBA $CCN_{0.2\%}$ are transported westward above the clouds and gradually enter the cloud layer from the cloud top, accompanying the increase of the marine boundary layer height and cloud height. These BBA could impact the cloud droplet number concentration either by acting as CCN or by evaporation of droplets through shortwave absorption. Although only a small fraction of the BBA associated to $CCN_{0.2\%}$ is contacted with cloud, the in-cloud $CCN_{0.2\%}$ can still reach up to ~ 500 cm-3, indicating the significant role of BBA acting as CCN and the potential impact upon the cloud and radiation balance through modulation of CDNC.

3.2.1 Biomass burning aerosols effects on cloud droplets

[insert ~~figure~~Fig. ~~4~~ 5 here]

The July and August averaged profile of BBA radiative and microphysical effects on maximum supersaturation~~n (SS)~~, as diagnosed by the activation scheme, from 2016 to 2017 are illustrated in ~~figure~~Fig. ~~3~~4. BBA slightly increase the maximum supersaturation ~~SS~~ near the continent and at low altitude over the SEA, while decrease the maximum supersaturation ~~SS~~ at the higher altitude. The increased maximum supersaturation ~~SS~~ mainly results from the BBA absorption effect, as the supersaturation ~~SS~~ profile is shifted to a lower altitude over the ocean. This maximum supersaturation ~~SS~~ altitude shift may be related to the change of the MBL height (~~Fig~~Fig.~~ure~~ S4). When BBA accumulates above the inversion the absorbed shortwave radiation warms the air at the bottom of the inversion layer, strengthening the temperature inversion (Fig. S5) and decreasing the MBL height. This is also supported by a radiosonde research (Adebiyi et al., 2015), which also found a shoaling of the boundary layer when absorbing aerosol was above. This effect is especially notable further away from the continent, where the MBL is also higher and sensitive to the temperature profile variations. Near the coast, BBA are generally above the underlying cloud deck; the absorption aerosols could strengthen the boundary layer inversion (Fig. S4) and thus decrease the dry air entrainment resulting in increased humidity and hence maximum supersaturation~~SS~~. The increased maximum supersaturation ~~SS~~ due to BBA absorption can be up to 53 % of the total ~~SS~~, indicating the significant role of the BBA absorption on the cloud droplet formation. The BBA scattering has little impact on ~~the~~ maximum supersaturation~~SS~~, with the mean effect around 0. The microphysical effect of BBA always exerts a negative impact on ~~the~~ maximum supersaturation~~SS~~, as expected from BBA acting as a condensation sink through hygroscopic growth or CCN activation and subsequent droplet growth. However, the decrease of the maximum supersaturation ~~SS~~ due to the BBA microphysical effect is comparatively small, indicating that the ability of BBA acting as CCN in our simulations is limited by its low hygroscopicity. In general, the BBA total effect on ~~the~~ maximum supersaturation ~~SS~~ shares a similar pattern with the absorption effect. However, as the BBA radiative and microphysical effect counterbalance in the lower part of the cloud, the total BBA effect on maximum supersaturation ~~SS~~ is smaller near the continent and at the cloud base. The ~~decrease~~ increase ~~of~~ in the maximum supersaturation ~~SS~~ from the BBA total effect is still quite noticeable.

[insert ~~figure~~Fig. ~~5~~ 6 here]

Before the onset of collision coalescence CDNC is determined by both the CCN and maximum supersaturation~~SS~~, and the variation of CDNC due to BBA is shown in ~~figure~~Fig. ~~5~~6. As illustrated through the previous analysis, although the radiative properties of BBA are not directly related to the CCN number concentration, this could still alter ~~the~~ maximum supersaturation ~~SS~~ and hence impact the activation of CCN. The change in CDNC due to the absorption of BBA shows a corresponding response to the effect of BBA on maximum supersaturation~~SS~~; shifting to lower altitude over the ocean, which expressed as increasing at the cloud base and decreasing at the cloud top over the ocean compare to the baseline simulation. Interestingly, the BBA absorption increases CDNC up to 102 cm^{-3} near the continent, which is surprisingly high as the maximum supersaturation ~~SS~~ only increases 0.152% by the absorption. This may partly be because the increased cloud fraction near the continent caused by the stabilising effect of absorption results in the increase of total CDNC; or the critical supersaturation of ambient aerosols is around the cloud maximum supersaturation~~SS~~, thus a slight variation of the cloud supersaturation would activate large amount of CCN. Unlike the effect of BBA absorption, the increased CDNC due to the microphysical effect is more notable over the sea, because only when the BBA are entrained and interact with the cloud, it can be activated as cloud droplets. The scattering effect only slightly increases CDNC when the MBL is deep enough to entrain BBA ~~(Fig.3)~~. However, similarly to the BBA scattering effect on maximum supersaturation~~SS~~, the increased CDNC due to scattering is negligible. In general, the substantial increase of CDNC by BBA can be attributed to the combined effect of absorption and microphysics, where the former mainly increases CDNC near the continent and at the lower altitude, and the latter increases CDNC above the ocean. Though BBA can contribute up to 56% of total CDNC in some areas, its average contribution during July to August in the SEA is around 13%, much less than its contribution to the $CCN_{0.2\%}$ budget fraction~~BBA contribute up to 56% of total~~ . This indicates a contribution of BBA above the cloud layer, unable to activate, although they can serve as CCN at 0.2% supersaturation~~CDNC (Figure S6), which is less than the fraction of $CCN_{0.2\%}$ it contributed.~~ . ~~This may indicate the maximum supersaturation achieved in the clouds is lower than 0.2% and most transported BBA have a small diameter; thus, the actual activated BBA are less than could be expected. However, the BBA attributed CDNC is still more than half, which confirm the primary source for the cloud droplets is biomass burning in this region.~~

3.2.2 Biomass burning aerosols effects on cloud liquid water

[insert ~~figure~~Fig. ~~6~~ 7 here]

The simulated changes of LWP in ~~figure~~Fig. ~~6~~ 7 shows a distinct response to BBA over the SEA. Within the cloud box area, the BBA interaction can increase LWP by up to ~34% of the total (~~Fig~~Fig. 3~~ure S7~~), indicating the critical influence of BBA on the stratocumulus deck. Figure ~~6~~ 7 shows that the BBA impacts the LWP mainly through its absorption effect. The increased LWP due to BBA absorption is more significant near the continent than in other areas, which may be because most BBA are above cloud near the continent. This finding is consistent with the result of ~~the~~ large-eddy simulations researches ~~by~~ (Herbert et al., 2020; Johnson et al., 2004; Yamaguchi et al., 2015; Zhou et al., 2017)~~Johnson et al. (2004)~~ that above cloud BBA can inhibit cloud-top entrainment and increase LWP. When BBA is transported further from the continent, the entrainment of BBA into the cloud layer reduces cloud droplet~~s~~ numbers by lowering the relative humidity through diabatic heating from absorption~~its absorption effect~~, which further reduces the increase of LWP, and results in a nearly zero or slightly negative effect on LWP. As a result of the different effects of the absorption by BBA as well as its spatial distribution (more concentrated near the continent), the increased LWP from BBA absorption is mainly located near the continent where the BBA and clouds are well separated, ~~the LWP from BBA absorption shows a steady negative gradient from west to east,~~ indicating the role of BBA in modulating the cloud distribution. The microphysical effect of BBA, which is less clearly distinguishable, generally increases the LWP above the ocean. However, the increase of LWP by the BBA microphysical effect in the cloud box only accounts for ~ 4% of the total LWP, far less than the BBA absorption effect. Therefore, the BBA effect on the LWP is mainly due to its absorption characteristics.

3.2.3 Biomass burning aerosols effect on cloud albedo

[insert ~~figure~~Fig. ~~7~~ 8 here]

Cloud albedo is crucial in climate, as it is one of the critical parameters in determining the shortwave cloud radiative effect. In the UKESM1, cloud albedo is diagnosed by the International Satellite Cloud Climatology Project (ISCCP) simulator (Bodas-Salcedo et al., 2011), which can minimize the impacts of how clouds are defined in different parameterizations and facilitate model intercomparison. As shown in ~~figure~~Fig. ~~7~~8, BBA generally increases cloud albedo in the cloud box area (total effect), which is consistent with relationships derived from a satellite based analysis (Deaconu et al., 2019). The cloud albedo increased by BBA account for ~8% of the total in the area where the stratocumulus cloud deck dominates (cloud box area) (~~Fig~~Fig.~~ure S8~~3). The effect of BBA on cloud albedo from BBA can be primarily attributed to absorption and the microphysical effect; these two effects together can account for the ~90 % of the cloud albedo increase due to BBA in the cloud box area. Unlike the microphysical effect, BBA absorption significantly increases cloud albedo near the continent where most BBA are above the cloud. The above cloud BBA can decrease the dry air entrainment and increase the liquid water content due to absorption (cf. ~~Fig.~~Fig. ~~6~~7), and lead to an increase in cloud particles and higher cloud albedo. However, when more BBA are entrained into the MBL, the BBA decrease the number of cloud droplets through its absorption effect and therefore, have a negative impact on the cloud albedo. Therefore, the two different effects of BBA absorption – BBA above clouds and inside clouds – counteract each other and result in a slight increase of LWP and a near-zero impact on the cloud albedo near the western boundary of the cloud box. Note that the LWP and the cloud albedo changes are consistent, although the different colour scale and the non-linear response of cloud albedo to LWP may result in the cloud albedo having less variation than the LWP in the western boundary of the cloud box. The microphysical effect of BBA increases cloud albedo homogenously over the ocean, because the increase of CCN provided by BBA increases CDNC. Compared to the effect of BBA absorption, the increased cloud albedo due to a change in CCN is small, indicating again the significant role of the BBA radiative properties.

3.3 Biomass burning aerosols radiative effect

[insert ~~figure~~Fig. ~~8~~ 9 here]

The time-averaged BBA effects on the top-of-atmosphere radiation balance are investigated in this section. The simulated direct radiative effect of BBA generally is positive, except in the western areas of the ocean (northwest of Ascension Island), where the BBA have transported far away from its source. The different sign of the mean direct effect depends on the underlying surface brightness; thus, when BBA are above clouds, the direct effect shows a warming effect while, when at clear sky, far away from the continent, it shows a cooling effect. However, the cooling due to the direct effect is negligible, as only a minor proportion of BBA with small particle diameters are transported so far west. The July-August averaged warming effect from the direct effect is large in the cloud box area: up to ~25.5 W m^{-2} near the continent. The indirect radiative effect of BBA shows a similar pattern to the LWP changes due to the microphysical effect of BBA, and has a July-August mean cooling effect of -1.2 W m^{-2} in the cloud box area. In some areas, the indirect effect shows a slight warming effect, which may be caused by the weather noise unconstrained by nudging between different initializations, as the cloud fraction and LWP both increase~~which may be due to the variation of meteorological conditions such as free-tropospheric humidity and lower tropospheric stability, as these can have prominent effects upon the magnitude and the sign of indirect effect (Ackerman et al., 2004; Chen et al., 2014)~~. The magnitude of the indirect effect is strongly related to the CCN; particles with high hygroscopicity could further increase the CDNC. Thus, different settings of OC hygroscopicity would result in differences in the indirect effect. In this paper, we use a kappa value of 0.3 for OC, which may account for some of the uncertainty in the indirect effect.

The BBA semi-direct radiative effects show the most substantial cooling in the cloud box; however, they also have a warming effect in the northwest areas over the sea outside the cloud box. The July-August semi-direct effects can be up to ~ -52 W m^{-2} near the coast, and dominate the total radiative effect in the cloud box area. The cooling of the semi-direct effects is mainly located in the area where the BBA are above the clouds and results from the significant increase of LWP and cloud albedo in that area (due to the stabilising effect of BBA absorption). The warming effect dominates where the cloud fraction is low, and BBA have already entered the boundary layer, which further reduced the cloud fraction and leads to the positive semi-direct effects. Thus, as the dominant effect over the Southeast Atlantic, the magnitude and the sign of the semi-direct effects are strongly dependent on the relative location of the BBA and the cloud layer. Herbert et al., (2020) studied different layers of the plume with different altitudes, and find out the closer the aerosols layer to the cloud top, the stronger the magnitude of the semi-direct effects. However, in our simulation, the BBA plume is not well separated from the underlying clouds. Thus, when the ~~absorption aerosols~~ BBA are closer to the cloud, some BBA may have entered the cloud layer. As a result, the above-cloud semi-direct effects lead to a top-of-atmosphere (TOA) cooling, whereas in-cloud semi-direct effects lead to a TOA warming.~~The semi-direct effects is resulted from both above cloud cooling and below cloud warming.~~

The total net radiative effect of the BBA shows a similar spatial pattern to the semi-direct effects albeit with a smaller magnitude, reflecting the dominant role of the semi-direct effects in this region. The total July-August BBA radiative effect over the whole domain is -0.9 Wm^{-2}, exerting a net cooling effect in that area. In the cloud box, the July-August averaged BBA total radiative effect can up to -30 Wm^{-2}, with a mean value of -5.7 Wm^{-2}. Gordon et al. (2018) have previously estimated the BBA radiative effects near Ascension Island using the same model with a different high-resolution configuration and model version. Comparing the radiative effects in the same domain, the direct and semi-direct effects from their simulations (direct effect: 10.3 Wm^{-2} and semi-direct effects: -16.1 Wm^{-2}) are roughly two times higher than our results (direct effect: 3.3 Wm^{-2} and semi-direct effects: -9.2 Wm^{-2}), as they only sampled the five most polluted days. ~~The direct and semi-direct effects show good agreement between our simulations and their findings; however, their results (direct effect: 10.3 Wm^{-2} and semi-direct effects: -16.1 Wm^{-2}) are slightly higher than our simulated cloud box mean values, as they only sampled the five most polluted days during their simulations.~~ Nevertheless, the indirect effect in their results is -11.4 Wm^{-2}, which is disproportionately ~~much~~ higher than our simulation (-0.6 Wm^{-2}). The possible reason behind this discrepancy is that the OC kappa value in their simulation is 0.88, which is much higher than our setting of 0.3. Furthermore, the meteorological conditions are different as they only averaged five days.

[insert ~~figure~~Fig. ~~9~~ 10 here]

The mean BBA radiative effects in the shortwave and longwave are summarised in ~~the figure~~Fig.~~.~~ ~~9~~10. In the cloud box, the semi-direct effects are the dominate BBA radiative effect, resulting in a considerable cooling of the total radiative effect over the cloud area. The cooling of semi-direct effects in the cloud box is generally at the shortwave, while at longwave, semi-direct effects show a slight warming effect. This may result from the semi-direct ~~effects~~ enhancement of LWP and cloud cover~~,~~ ; ~~which would~~therefore, the outgoing longwave radiation at the top of the atmosphere is reduced as it comes from the relatively cool cloud tops rather than the warmer ocean ~~further increase the sunlight reflection as well as the absorption of longwave radiation from the underlying warmer surface. The~~surface, as discussed in ~~(~~Zhou et al.~~,~~ (2017). The direct effect is 7 Wm^{-2} in the cloud box area, which partially cancels the cooling of the semi-direct effects. The indirect effect is cooling in this area. However, its magnitude is relatively small, which may be result~~eds~~ from the limited capability of BBA in acting as CCN due to its low hygroscopicity.

For the regional domain, the BBA semi-direct effects also show a negative cooling effect. However, compared with the cloud box, the mean value of semi-direct effects decreases rapidly when the averaged domain size increases, as it is only about -1.6 W m^{-2} for the regional domain, i.e. ~ 13% of the semi-direct net effects in the cloud box area. Globally, the net semi-direct effects are nearly zero, indicating the semi-direct effects from biomass burning primarily affect the cloud deck over the SEA. The regional averaged indirect effect is similar to the cloud box mean, and slightly lower than the regional semi-direct effects, indicating the role of the BBA cloud interactions in this region. In general, BBA have the most significant radiative effects in the cloud deck area, followed by in the South Atlantic Ocean and west African (regional domain). The indirect effect is generally the same in these areas and is one of the critical factors in determining the regional radiation balance. The dominant effect in these areas is the cooling effect exerted by the semi-direct radiative effects.

Discussion and conclusion

The UK Earth System Model (UKESM1) is used to investigate the effects of biomass burning aerosols over the southeast Atlantic to provide both a better understanding of their radiative and microphysical effects on clouds, and the radiation balance in this area. The analysis focuses on the biomass burning seasons from July to August for the years 2016 and 2017, which facilitates model evaluation with flight measurements from the ORACLES and CLARIFY measurement campaigns.

Comparison with the flight observations shows that the model generally captures the spatial and vertical distributions of BBA plume; however, the simulated plume is located too far north-west and at a slightly lower altitude in the model. Although the semi-direct effects and cloud response are sensitive to the relative distance of cloud and biomass burning plume (Herbert et al., 2020), these errors are relatively small, providing the foundation for our investigation of the BBA effect on clouds and the radiation balance in this region.

The BBA associated CCN are emitted from the land and then transported westward above the cloud. With the increase of the marine boundary layer height, and reduction of the plume height, BBA enter the cloud layer from the top. The budget of $CCN_{0.2\%}$ attributable to BBA can account for ~ 65~~8~~% of the total $CCN_{0.2\%}$ in the cloud box area, indicating that BBA are the primary source of CCN for the marine stratocumulus deck.

The effects of BBA on clouds are separated into radiative effects (including the effects from absorption and scattering) and the microphysical effect. The impact of BBA on in-cloud maximum supersaturation is mainly due to its absorption. When BBA accumulate above the inversion, the absorbed shortwave radiation warms the air at the bottom of the inversion layer, strengthening ~~lowering~~ the temperature inversion and decreasing the marine boundary layer height. As a consequence, the maximum supersaturation shifts to a lower altitude above the ocean. Near the coast, the above cloud BBA strengthens the temperature inversion, which results in the weakening of the entrainment across the inversion layer, as buoyant parcels of air in the MBL require more energy in order to push through the strengthened temperature inversion (Herbert et al., 2020). Therefore, the relative humidity increases, as well as the supersaturation. As a consequence, the BBA absorption effect shows a corresponding response: increases at low altitudes (cloud bottom in baseline simulation) and decrease at high altitudes (cloud top from baseline) over the ocean further offshore, and generally increases near the continent. The microphysical effect decreases the maximum supersaturation, as BBA can act as CCN and allow additional water vapour to condense; however, this decrease is comparatively small ~~in this area~~. The CDNC over SEA is increased especially further offshore due to ~~Due to the shift of maximum supersaturation by BBA absorption the CDNC shows a corresponding response: increasing at low~~

~~altitudes (cloud bottom in baseline simulations) and decreasing at high altitudes (cloud top from baseline) over the ocean. However,~~ the BBA microphysical effect, compensating the decreased CDNC at the higher altitude from the absorption effect. In general, BBA absorption and microphysical effects both contribute to the increase of CDNC, although the former is mainly through affecting the maximum supersaturation while the latter is through increasing CCN. ~~increases CDNC further from the continent, cancelling out the decreases from absorption. The CDNC attributed to BBA can be up to 56% of total CDNC, confirming the significant impact of BBA on the cloud deck.~~

The BBA absorption effect increases LWP significantly when BBA are located above the stratocumulus deck, as the stabilisation from absorption can inhibit cloud-top entrainment. When BBA enter the cloud layer, it can decrease the amount of condensable liquid water and so decrease the LWP. As a result, the variation of LWP due to the absorption effect is nearly zero or slightly negative when far away from the continent. The microphysical effect also contributes to the increase in LWP; however, this increase is small compare to the absorption effect. Therefore, the LWP response to BBA is dominated by the effect of absorption, showing a substantial increase over the Southeast Atlantic. The variation of cloud albedo due to BBA shows a similar pattern to the LWP.

The dominance of the effect of absorption on cloud properties is reflected in the effect on the top-of-atmosphere radiation balance. When the BBA are above the stratocumulus deck, semi-direct effects contribute most to the overall cooling, while they also exert a warming effect in the northwest areas over the sea. The magnitude and the sign of the semi-direct effects are dependent on the relative location of BBA and clouds, as BBA can either increase the underlying cloud LWP or decrease the surrounding droplet numbers depending on whether the BBA are above or inside the cloud. The direct radiative effect is generally positive and shows a strong warming when BBA are above the stratocumulus deck (with July-August average 7.5 W m^{-2}), as the surface albedo of the underlying clouds is fairly high. However, for the total net BBA radiative effect the positive direct radiative effect is more than compensated by the semi-direct effects, resulting in an overall cooling effect over the SEA (with July-August average -0.9 W m^{-2}). In addition to the semi-direct effects, the indirect radiative effect is also negative, showing a cooling in this area. The indirect effect mainly results from the response of LWP to the BBA microphysical effect, as they share a similar spatial pattern. When comparing the BBA radiative effects at different scales, we find that semi-direct effects from biomass burning play a significant role over the southeast Atlantic stratocumulus deck, while it has little impact in the global mean. ~~The indirect effect from biomass burning aerosol, however, have a similar magnitude in both regional and global, showing a more widespread cooling effect.~~

Data availability

The original simulation data are available from JASMIN facility upon request. There is also processed model data, which can be downloaded from https://data.mendeley.com/datasets/xdxh8stc48/2. Data from the CLARIFY aircraft campaign are available on the CEDA repository http://archive.ceda.ac.uk/. Data from ORACLES aircraft campaigns are available on the repository https://espo.nasa.gov/oracles/archive/browse/oracles.

Author contributions

PS and HC developed the concepts and ideas for the direction of the paper. HC and HG set up the model. HC carried out and analysed the model simulation. DWP and HC performed the model validation, LD, DWP, HG, HC and PS contributed the analysis of the results. HC wrote the paper with input and comments from all other authors.

Competing interests

The authors declare that they have no conflict of interest.

Special issue statement.

This article is part of the special issue "New observations and related modelling studies of the aerosol- cloud-climate system in the Southeast Atlantic and southern Africa regions (ACP/AMT inter-journal SI)". It is not associated with a conference.

Acknowledgements

This research has been funded by the NERC CLARIFY project NE/L013479/1. P.S. additionally acknowledges support from the European Research Council (ERC) project constRaining the EffeCts of Aerosols on Precipitation (RECAP) under the European Union's Horizon 2020 research and innovation program with grant agreement 724602. We sincerely acknowledge Kate Szpek from Met Office CLARIFY team, and Steven Howell from NASA ORACLES team for providing aerosols scattering and absorption data, and all CLARIFY and ORACLES science teams for data support. We also thanks Luke Abraham and William Ingram for the help with the model, Ben Johnson for the help of setting up biomass burning emissions, William Jones for proofreading the manuscript. We acknowledge the use of the Monsoon2 system, a collaborative facility supplied under the Joint Weather and Climate Research Programme, a strategic partnership between the UK Met Office and the Natural Environment Research Council (NERC). We also used the JASMIN facility (http://www.jasmin.ac.uk/) via the Centre for Environmental Data Analysis, funded by NERC and the UK Space Agency and delivered by the Science and Technology Facilities Council.

References

Ackerman, A. S., Kirkpatrick, M. P., Stevens, D. E. and Toon, O. B.: The impact of humidity above stratiform clouds on indirect aerosol climate forcing, Nature, 432(7020), 1014, doi:10.1038/nature03174, 2004.

Adebiyi, A. A. and Zuidema, P.: The role of the southern African easterly jet in modifying the southeast Atlantic aerosol and cloud environments, Quarterly Journal of the Royal Meteorological Society, 142(697), 1574–1589, doi:10.1002/qj.2765, 2016.

Adebiyi, A. A., Zuidema, P. and Abel, S. J.: The Convolution of Dynamics and Moisture with the Presence of Shortwave Absorbing Aerosols over the Southeast Atlantic, J. Climate, 28(5), 1997–2024, doi:10.1175/JCLI-D-14-00352.1, 2015.

Bellouin, N., Quaas, J., Gryspeerdt, E., Kinne, S., Stier, P., Watson-Parris, D., Boucher, O., Carslaw, K. S., Christensen, M., Daniau, A.-L., Dufresne, J.-L., Feingold, G., Fiedler, S., Forster, P., Gettelman, A., Haywood, J. M., Lohmann, U., Malavelle, F., Mauritsen, T., McCoy, D. T., Myhre, G., Mülmenstädt, J., Neubauer, D., Possner, A., Rugenstein, M., Sato, Y., Schulz, M., Schwartz, S. E., Sourdeval, O., Storelvmo, T., Toll, V., Winker, D. and Stevens, B.: Bounding global aerosol radiative forcing of climate change, Reviews of Geophysics, n/a(n/a), doi:10.1029/2019RG000660, 2019.

Bodas-Salcedo, A., Webb, M. J., Bony, S., Chepfer, H., Dufresne, J.-L., Klein, S. A., Zhang, Y., Marchand, R., Haynes, J. M., Pincus, R. and John, V. O.: COSP: Satellite simulation software for model assessment, Bull. Amer. Meteor. Soc., 92(8), 1023–1043, doi:10.1175/2011BAMS2856.1, 2011.

Chand, D., Wood, R., Anderson, T. L., Satheesh, S. K. and Charlson, R. J.: Satellite-derived direct radiative effect of aerosols dependent on cloud cover, Nature Geoscience, 2(3), 181–184, doi:10.1038/ngeo437, 2009.

Chang, R. Y.-W., Slowik, J. G., Shantz, N. C., Vlasenko, A., Liggio, J., Sjostedt, S. J., Leaitch, W. R. and Abbatt, J. P. D.: The hygroscopicity parameter (κ) of ambient organic aerosol at a field site subject to biogenic and anthropogenic influences: relationship to degree of aerosol oxidation, Atmos. Chem. Phys., 10(11), 5047–5064, doi:10.5194/acp-10-5047-2010, 2010.

Costantino, L. and Bréon, F.-M.: Analysis of aerosol-cloud interaction from multi-sensor satellite observations, Geophysical Research Letters, 37(11), doi:10.1029/2009GL041828, 2010.

Costantino, L. and Bréon, F.-M.: Aerosol indirect effect on warm clouds over South-East Atlantic, from co-located MODIS and CALIPSO observations, Atmospheric Chemistry and Physics, 13(1), 69–88, doi:https://doi.org/10.5194/acp-13-69-2013, 2013.

Cotterell, M. I., Szpek, K., Haywood, J. M. and Langridge, J. M.: Sensitivity and accuracy of refractive index retrievals from measured extinction and absorption cross sections for mobility-selected internally mixed light absorbing aerosols, Aerosol Science and Technology, 54(9), 1034–1057, doi:10.1080/02786826.2020.1757034, 2020.

Davies, N. W., Cotterell, M. I., Fox, C., Szpek, K., Haywood, J. M. and Langridge, J. M.: On the accuracy of aerosol photoacoustic spectrometer calibrations using absorption by ozone, Atmospheric Measurement Techniques, 11(4), 2313–2324, doi:https://doi.org/10.5194/amt-11-2313-2018, 2018.

Deaconu, L. T., Ferlay, N., Waquet, F., Peers, F., Thieuleux, F. and Goloub, P.: Satellite inference of water vapor and aerosol-above-cloud combined effect on radiative budget and cloud top processes in the Southeast Atlantic Ocean, Atmospheric Chemistry and Physics Discussions, 1–34, doi:https://doi.org/10.5194/acp-2019-189, 2019.

Diamond, M. S., Dobracki, A., Freitag, S., Small Griswold, J. D., Heikkila, A., Howell, S. G., Kacarab, M. E., Podolske, J. R., Saide, P. E. and Wood, R.: Time-dependent entrainment of smoke presents an observational challenge for assessing aerosol–

cloud interactions over the southeast Atlantic Ocean, Atmospheric Chemistry and Physics, 18(19), 14623–14636, doi:https://doi.org/10.5194/acp-18-14623-2018, 2018.

Eyring, V., Bony, S., Meehl, G. A., Senior, C. A., Stevens, B., Stouffer, R. J. and Taylor, K. E.: Overview of the Coupled Model Intercomparison Project Phase 6 (CMIP6) experimental design and organization, Geoscientific Model Development, 9(5), 1937–1958, doi:https://doi.org/10.5194/gmd-9-1937-2016, 2016.

Ghan, S. J., Liu, X., Easter, R. C., Zaveri, R., Rasch, P. J., Yoon, J.-H. and Eaton, B.: Toward a Minimal Representation of Aerosols in Climate Models: Comparative Decomposition of Aerosol Direct, Semidirect, and Indirect Radiative Forcing, J. Climate, 25(19), 6461–6476, doi:10.1175/JCLI-D-11-00650.1, 2012.

Gidden, M. J., Riahi, K., Smith, S. J., Fujimori, S., Luderer, G., Kriegler, E., Vuuren, D. P. van, Berg, M. van den, Feng, L., Klein, D., Calvin, K., Doelman, J. C., Frank, S., Fricko, O., Harmsen, M., Hasegawa, T., Havlik, P., Hilaire, J., Hoesly, R., Horing, J., Popp, A., Stehfest, E. and Takahashi, K.: Global emissions pathways under different socioeconomic scenarios for use in CMIP6: a dataset of harmonized emissions trajectories through the end of the century, Geoscientific Model Development, 12(4), 1443–1475, doi:https://doi.org/10.5194/gmd-12-1443-2019, 2019.

Gordon, H., Field, P. R., Abel, S. J., Dalvi, M., Grosvenor, D. P., Hill, A. A., Johnson, B. T., Miltenberger, A. K., Yoshioka, M. and Carslaw, K. S.: Large simulated radiative effects of smoke in the south-east Atlantic, Atmospheric Chemistry and Physics, 18(20), 15261–15289, doi:https://doi.org/10.5194/acp-18-15261-2018, 2018.

Hansen, J., Sato, M. and Ruedy, R.: Radiative forcing and climate response, Journal of Geophysical Research: Atmospheres, 102(D6), 6831–6864, 1997.

Haywood, J. M., Abel, S. J., Barrett, P. A., Bellouin, N., Blyth, A., Bower, K. N., Brooks, M., Carslaw, K., Che, H., Coe, H., Cotterell, M. I., Crawford, I., Cui, Z., Davies, N., Dingley, B., Field, P., Formenti, P., Gordon, H., de Graaf, M., Herbert, R., Johnson, B., Jones, A. C., Langridge, J. M., Malavelle, F., Partridge, D. G., Peers, F., Redemann, J., Stier, P., Szpek, K., Taylor, J. W., Watson-Parris, D., Wood, R., Wu, H. and Zuidema, P.: Overview: The CLoud-Aerosol-Radiation Interaction and Forcing: Year-2017 (CLARIFY-2017) measurement campaign, Atmospheric Chemistry and Physics Discussions, 1–49, doi:https://doi.org/10.5194/acp-2020-729, 2020.

Herbert, R. J., Bellouin, N., Highwood, E. J. and Hill, A. A.: Diurnal cycle of the semi-direct effect from a persistent absorbing aerosol layer over marine stratocumulus in large-eddy simulations, Atmospheric Chemistry and Physics, 20(3), 1317–1340, doi:https://doi.org/10.5194/acp-20-1317-2020, 2020.

Hewitt, H. T., Copsey, D., Culverwell, I. D., Harris, C. M., Hill, R. S. R., Keen, A. B., McLaren, A. J. and Hunke, E. C.: Design and implementation of the infrastructure of HadGEM3: the next-generation Met Office climate modelling system, Geoscientific Model Development, 4(2), 223–253, doi:https://doi.org/10.5194/gmd-4-223-2011, 2011.

Hill, A. A., Dobbie, S. and Yin, Y.: The impact of aerosols on non-precipitating marine stratocumulus. I: Model description and prediction of the indirect effect, Quarterly Journal of the Royal Meteorological Society, 134(634), 1143–1154, doi:10.1002/qj.278, 2008.

Hobbs, P. V.: Clean air slots amid atmospheric pollution, Nature, 415(6874), 861, doi:10.1038/415861a, 2002.

Johnson, B. T., Shine, K. P. and Forster, P. M.: The semi-direct aerosol effect: Impact of absorbing aerosols on marine stratocumulus, Quarterly Journal of the Royal Meteorological Society, 130(599), 1407–1422, doi:10.1256/qj.03.61, 2004.

Johnson, B. T., Haywood, J. M., Langridge, J. M., Darbyshire, E., Morgan, W. T., Szpek, K., Brooke, J. K., Marenco, F., Coe, H., Artaxo, P., Longo, K. M., Mulcahy, J. P., Mann, G. W., Dalvi, M. and Bellouin, N.: Evaluation of biomass burning aerosols in the HadGEM3 climate model with observations from the SAMBBA field campaign, Atmospheric Chemistry and Physics, 16(22), 14657–14685, doi:https://doi.org/10.5194/acp-16-14657-2016, 2016.

Kacarab, M., Thornhill, K. L., Dobracki, A., Howell, S. G., O'Brien, J. R., Freitag, S., Poellot, M. R., Wood, R., Zuidema, P., Redemann, J. and Nenes, A.: Biomass burning aerosol as a modulator of the droplet number in the southeast Atlantic region, Atmospheric Chemistry and Physics, 20(5), 3029–3040, doi:https://doi.org/10.5194/acp-20-3029-2020, 2020.

Kaiser, J.W., Heil, A., Andreae, M.O., Benedetti, A., Chubarova, N., Jones, L., Morcrette, J.J., Razinger, M., Schultz, M.G., Suttie, M., van der Werf, G.R., Earth and Climate and Amsterdam Global Change Institute: Biomass burning emissions estimated with a global fire assimilation system based on observed fire radiative power, Biogeosciences, 9(1), 527–554, doi:10.5194/bg-9-527-2012, 2012.

Koch, D. and Genio, A. D. D.: Black carbon semi-direct effects on cloud cover: review and synthesis, Atmospheric Chemistry and Physics, 10(16), 7685–7696, doi:https://doi.org/10.5194/acp-10-7685-2010, 2010.

Langridge, J. M., Richardson, M. S., Lack, D., Law, D. and Murphy, D. M.: Aircraft Instrument for Comprehensive Characterization of Aerosol Optical Properties, Part I: Wavelength-Dependent Optical Extinction and Its Relative Humidity Dependence Measured Using Cavity Ringdown Spectroscopy, Aerosol Science and Technology, 45(11), 1305–1318, doi:10.1080/02786826.2011.592745, 2011.

Lu, Z., Liu, X., Zhang, Z., Zhao, C., Meyer, K., Rajapakshe, C., Wu, C., Yang, Z. and Penner, J. E.: Biomass smoke from southern Africa can significantly enhance the brightness of stratocumulus over the southeastern Atlantic Ocean, PNAS, 115(12), 2924–2929, doi:10.1073/pnas.1713703115, 2018.

Mann, G. W., Carslaw, K. S., Spracklen, D. V., Ridley, D. A., Manktelow, P. T., Chipperfield, M. P., Pickering, S. J. and Johnson, C. E.: Description and evaluation of GLOMAP-mode: a modal global aerosol microphysics model for the UKCA composition-climate model, Geosci. Model Dev., 3(2), 519–551, doi:10.5194/gmd-3-519-2010, 2010.

Mulcahy, J. P., Johnson, C., Jones, C. G., Povey, A. C., Scott, C. E., Sellar, A., Turnock, S. T., Woodhouse, M. T., Abraham, N. L., Andrews, M. B., Bellouin, N., Browse, J., Carslaw, K. S., Dalvi, M., Folberth, G. A., Glover, M., Grosvenor, D., Hardacre, C., Hill, R., Johnson, B., Jones, A., Kipling, Z., Mann, G., Mollard, J., O'Connor, F. M., Palmieri, J., Reddington, C., Rumbold, S. T., Richardson, M., Schutgens, N. A. J., Stier, P., Stringer, M., Tang, Y., Walton, J., Woodward, S. and Yool, A.: Description and evaluation of aerosol in UKESM1 and HadGEM3-GC3.1 CMIP6 historical simulations, Submitted, 2020.

O'Connor, F. M., Johnson, C. E., Morgenstern, O., Abraham, N. L., Braesicke, P., Dalvi, M., Folberth, G. A., Sanderson, M. G., Telford, P. J., Voulgarakis, A., Young, P. J., Zeng, G., Collins, W. J. and Pyle, J. A.: Evaluation of the new UKCA climate-composition model – Part 2: The Troposphere, Geosci. Model Dev., 7(1), 41–91, doi:10.5194/gmd-7-41-2014, 2014.

Painemal, D., Kato, S. and Minnis, P.: Boundary layer regulation in the southeast Atlantic cloud microphysics during the biomass burning season as seen by the A-train satellite constellation, Journal of Geophysical Research: Atmospheres, 119(19), 11,288-11,302, doi:10.1002/2014JD022182, 2014.

Pistone, K., Redemann, J., Doherty, S., Zuidema, P., Burton, S., Cairns, B., Cochrane, S., Ferrare, R., Flynn, C., Freitag, S., Howell, S. G., Kacenelenbogen, M., LeBlanc, S., Liu, X., Schmidt, K. S., Sedlacek III, A. J., Segal-Rozenhaimer, M., Shinozuka, Y., Stamnes, S., Diedenhoven, B. van, Harten, G. V. and Xu, F.: Intercomparison of biomass burning aerosol optical properties from in situ and remote-sensing instruments in ORACLES-2016, Atmospheric Chemistry and Physics, 19(14), 9181–9208, doi:https://doi.org/10.5194/acp-19-9181-2019, 2019.

Redemann, J., Wood, R., Zuidema, P., Doherty, S. J., Luna, B., LeBlanc, S. E., Diamond, M. S., Shinozuka, Y., Chang, I. Y., Ueyama, R., Pfister, L., Ryoo, J., Dobracki, A. N., Silva, A. M. da, Longo, K. M., Kacenelenbogen, M. S., Flynn, C. J., Pistone, K., Knox, N. M., Piketh, S. J., Haywood, J. M., Formenti, P., Mallet, M., Stier, P., Ackerman, A. S., Bauer, S. E., Fridlind, A. M., Carmichael, G. R., Saide, P. E., Ferrada, G. A., Howell, S. G., Freitag, S., Cairns, B., Holben, B. N., Knobelspiesse, K. D., Tanelli, S., L'Ecuyer, T. S., Dzambo, A. M., Sy, O. O., McFarquhar, G. M., Poellot, M. R., Gupta, S., O'Brien, J. R., Nenes, A., Kacarab, M. E., Wong, J. P. S., Small-Griswold, J. D., Thornhill, K. L., Noone, D., Podolske, J. R., Schmidt, K. S., Pilewskie, P., Chen, H., Cochrane, S. P., Sedlacek, A. J., Lang, T. J., Stith, E., Segal-Rozenhaimer, M., Ferrare, R. A., Burton, S. P., Hostetler, C. A., Diner, D. J., Platnick, S. E., Myers, J. S., Meyer, K. G., Spangenberg, D. A., Maring, H. and Gao, L.: An overview of the ORACLES (ObseRvations of Aerosols above CLouds and their intEractionS) project: aerosol-cloud-radiation interactions in the Southeast Atlantic basin, Atmospheric Chemistry and Physics Discussions, 1–82, doi:https://doi.org/10.5194/acp-2020-449, 2020.

Reynolds, R. W., Smith, T. M., Liu, C., Chelton, D. B., Casey, K. S. and Schlax, M. G.: Daily High-Resolution-Blended Analyses for Sea Surface Temperature, J. Climate, 20(22), 5473–5496, doi:10.1175/2007JCLI1824.1, 2007.

Ridley, J. K., Blockley, E. W., Keen, A. B., Rae, J. G. L., West, A. E. and Schroeder, D.: The sea ice model component of HadGEM3-GC3.1, Geoscientific Model Development, 11(2), 713–723, doi:https://doi.org/10.5194/gmd-11-713-2018, 2018.

Roberts, G., Wooster, M. J. and Lagoudakis, E.: Annual and diurnal african biomass burning temporal dynamics, Biogeosciences, 6(5), 849–866, doi:https://doi.org/10.5194/bg-6-849-2009, 2009.

Sakaeda, N., Wood, R. and Rasch, P. J.: Direct and semidirect aerosol effects of southern African biomass burning aerosol, Journal of Geophysical Research: Atmospheres, 116(D12), doi:10.1029/2010JD015540, 2011.

Sellar, A. A., Jones, C. G., Mulcahy, J. P., Tang, Y., Yool, A., Wiltshire, A., O'Connor, F. M., Stringer, M., Hill, R., Palmieri, J., Woodward, S., Mora, L. de, Kuhlbrodt, T., Rumbold, S. T., Kelley, D. I., Ellis, R., Johnson, C. E., Walton, J., Abraham, N. L., Andrews, M. B., Andrews, T., Archibald, A. T., Berthou, S., Burke, E., Blockley, E., Carslaw, K., Dalvi, M., Edwards, J., Folberth, G. A., Gedney, N., Griffiths, P. T., Harper, A. B., Hendry, M. A., Hewitt, A. J., Johnson, B., Jones, A., Jones, C. D., Keeble, J., Liddicoat, S., Morgenstern, O., Parker, R. J., Predoi, V., Robertson, E., Siahaan, A., Smith, R. S., Swaminathan, R., Woodhouse, M. T., Zeng, G. and Zerroukat, M.: UKESM1: Description and Evaluation of the U.K. Earth System Model, Journal of Advances in Modeling Earth Systems, 11(12), 4513–4558, doi:10.1029/2019MS001739, 2019.

Shinozuka, Y., Saide, P. E., Ferrada, G. A., Burton, S. P., Ferrare, R., Doherty, S. J., Gordon, H., Longo, K., Mallet, M., Feng, Y., Wang, Q., Cheng, Y., Dobracki, A., Freitag, S., Howell, S. G., LeBlanc, S., Flynn, C., Segal-Rosenhaimer, M., Pistone, K., Podolske, J. R., Stith, E. J., Bennett, J. R., Carmichael, G. R., Silva, A. da, Govindaraju, R., Leung, R., Zhang, Y., Pfister, L., Ryoo, J.-M., Redemann, J., Wood, R. and Zuidema, P.: Modeling the smoky troposphere of the southeast Atlantic: a comparison to ORACLES airborne observations from September of 2016, Atmospheric Chemistry and Physics Discussions, 1–77, doi:https://doi.org/10.5194/acp-2019-678, 2019.

Stier, P., Schutgens, N. a. J., Bellouin, N., Bian, H., Boucher, O., Chin, M., Ghan, S., Huneeus, N., Kinne, S., Lin, G., Ma, X., Myhre, G., Penner, J. E., Randles, C. A., Samset, B., Schulz, M., Takemura, T., Yu, F., Yu, H. and Zhou, C.: Host model uncertainties in aerosol radiative forcing estimates: results from the AeroCom Prescribed intercomparison study, Atmospheric Chemistry and Physics, 13(6), 3245–3270, doi:https://doi.org/10.5194/acp-13-3245-2013, 2013.

Storkey, D., Blaker, A. T., Mathiot, P., Megann, A., Aksenov, Y., Blockley, E. W., Calvert, D., Graham, T., Hewitt, H. T., Hyder, P., Kuhlbrodt, T., Rae, J. G. L. and Sinha, B.: UK Global Ocean GO6 and GO7: a traceable hierarchy of model resolutions, Geoscientific Model Development, 11(8), 3187–3213, doi:https://doi.org/10.5194/gmd-11-3187-2018, 2018.

Telford, P. J., Braesicke, P., Morgenstern, O. and Pyle, J. A.: Technical Note: Description and assessment of a nudged version of the new dynamics Unified Model, Atmos. Chem. Phys., 8(6), 1701–1712, doi:10.5194/acp-8-1701-2008, 2008.

Twomey, S.: Pollution and the planetary albedo, Atmos. Environ, 8(12), 1251–1256, 1974.

Twomey, S.: The influence of pollution on the shortwave albedo of clouds, Journal of the atmospheric sciences, 34(7), 1149–1152, 1977.

Walters, D., Baran, A., Boutle, I., Brooks, M., Earnshaw, P., Edwards, J., Furtado, K., Hill, P., Lock, A., Manners, J., Morcrette, C., Mulcahy, J., Sanchez, C., Smith, C., Stratton, R., Tennant, W., Tomassini, L., Weverberg, K. V., Vosper, S., Willett, M., Browse, J., Bushell, A., Dalvi, M., Essery, R., Gedney, N., Hardiman, S., Johnson, B., Johnson, C., Jones, A., Mann, G., Milton, S., Rumbold, H., Sellar, A., Ujiie, M., Whitall, M., Williams, K. and Zerroukat, M.: The Met Office Unified Model Global Atmosphere 7.0/7.1 and JULES Global Land 7.0 configurations, Geoscientific Model Development Discussions, 1–78, doi:https://doi.org/10.5194/gmd-2017-291, 2017.

Watson-Parris, D., Schutgens, N., Cook, N., Kipling, Z., Kershaw, P., Gryspeerdt, E., Lawrence, B. and Stier, P.: Community Intercomparison Suite (CIS) v1.4.0: a tool for intercomparing models and observations, Geoscientific Model Development, 9(9), 3093–3110, doi:https://doi.org/10.5194/gmd-9-3093-2016, 2016.

Watson-Parris, D., Schutgens, N., Reddington, C., Pringle, K. J., Liu, D., Allan, J. D., Coe, H., Carslaw, K. S. and Stier, P.: In-situ constraints on the vertical distribution of global aerosol, Atmospheric Chemistry and Physics Discussions, 1–48, doi:https://doi.org/10.5194/acp-2018-1337, 2019.

van der Werf, G. R., Randerson, J. T., Giglio, L., Collatz, G. J., Mu, M., Kasibhatla, P. S., Morton, D. C., DeFries, R. S., Jin, Y. and Leeuwen, T. T. van: Global fire emissions and the contribution of deforestation, savanna, forest, agricultural, and peat fires (1997–2009), Atmospheric Chemistry and Physics, 10(23), 11707–11735, doi:https://doi.org/10.5194/acp-10-11707-2010, 2010.

Wilcox, E. M.: Stratocumulus cloud thickening beneath layers of absorbing smoke aerosol, Atmospheric Chemistry and Physics, 10(23), 11769–11777, doi:https://doi.org/10.5194/acp-10-11769-2010, 2010.

Wilcox, E. M.: Direct and semi-direct radiative forcing of smoke aerosols over clouds, Atmospheric Chemistry and Physics, 12(1), 139–149, doi:https://doi.org/10.5194/acp-12-139-2012, 2012.

Wood, R.: Cancellation of Aerosol Indirect Effects in Marine Stratocumulus through Cloud Thinning, J. Atmos. Sci., 64(7), 2657–2669, doi:10.1175/JAS3942.1, 2007.

Wood, R.: Stratocumulus Clouds, Mon. Wea. Rev., 140(8), 2373–2423, doi:10.1175/MWR-D-11-00121.1, 2012.

Woodward, S.: Modeling the atmospheric life cycle and radiative impact of mineral dust in the Hadley Centre climate model, Journal of Geophysical Research: Atmospheres, 106(D16), 18155–18166, doi:10.1029/2000JD900795, 2001.

Yamaguchi, T., Feingold, G., Kazil, J. and McComiskey, A.: Stratocumulus to cumulus transition in the presence of elevated smoke layers, Geophysical Research Letters, 42(23), 10,478-10,485, doi:10.1002/2015GL066544, 2015.

Zhang, K., Wan, H., Liu, X., Ghan, S. J., Kooperman, G. J., Ma, P.-L., Rasch, P. J., Neubauer, D. and Lohmann, U.: Technical Note: On the use of nudging for aerosol–climate model intercomparison studies, Atmospheric Chemistry and Physics, 14(16), 8631–8645, doi:https://doi.org/10.5194/acp-14-8631-2014, 2014.

Zhou, X., Ackerman, A. S., Fridlind, A. M., Wood, R. and Kollias, P.: Impacts of solar-absorbing aerosol layers on the transition of stratocumulus to trade cumulus clouds, Atmospheric Chemistry and Physics, 17(20), 12725–12742, doi:https://doi.org/10.5194/acp-17-12725-2017, 2017.

Zuidema, P., Sedlacek, A. J., Flynn, C., Springston, S., Delgadillo, R., Zhang, J., Aiken, A. C., Koontz, A. and Muradyan, P.: The Ascension Island Boundary Layer in the Remote Southeast Atlantic is Often Smoky, Geophysical Research Letters, 45(9), 4456–4465, doi:10.1002/2017GL076926, 2018.

Figures

.

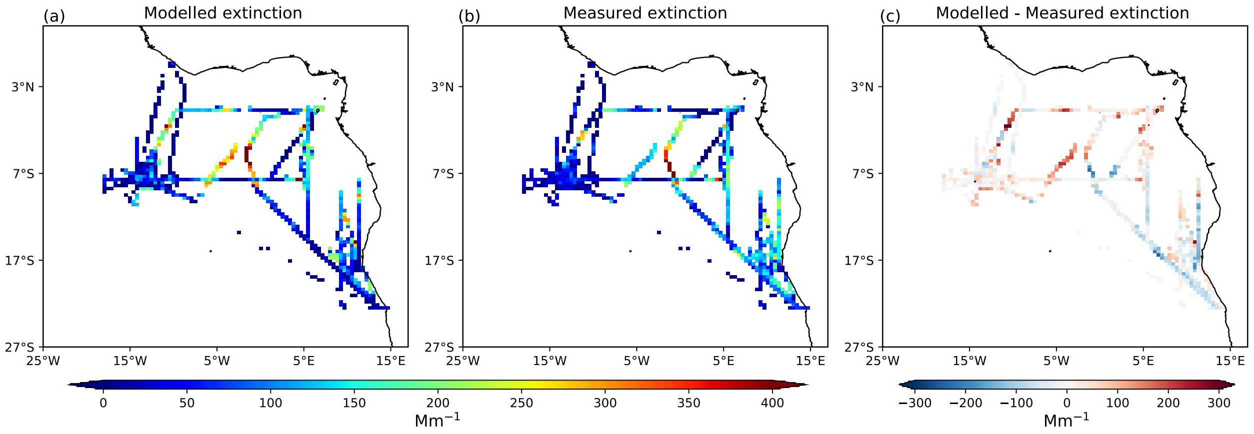

Figure 1: Mean along track aerosol extinction coefficient [Mm^{-1}] from the (a) UKESM1 model collocated to the flight tracks, (b) flight observations, and (c) differences between the model and observations. Note that the model extinction is under ambient conditions, whereas the measured extinction is for dry aerosols with relative humidity below 30%.

~~Figure 1: Mean (a) modelled and (b) measured aerosol extinction coefficient [Mm^{-1}] along the flight tracks and the (c) differences between model and measurement. Note that the model extinction is at ambient conditions whereas the measured extinction is for dry aerosols with relative humidity below 30%.~~

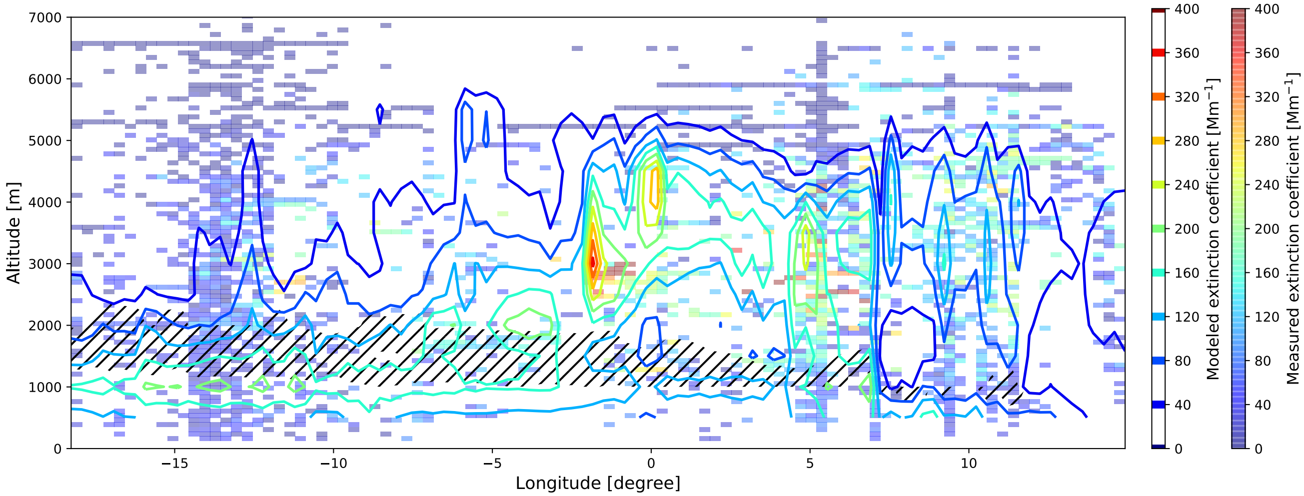

Figure 2. Mean along-flight track vertical distribution of the aerosol extinction coefficient along longitude. The contour lines show the mean collocated model extinction coefficient profile along with the location of the aircraft. The pixels represent the mean value of aerosol extinction coefficient from CLARIFY and ORACLES (2016, 2017) campaigns. The hashed lines illustrate the model cloud location by using cloud liquid water content from the model. Note that the modelled extinction is for ambient relative humidity whereas the measured extinction is for dry aerosols with relative humidity below 30%. The same colourmap is applied for measurement and model result to facilitate comparison.

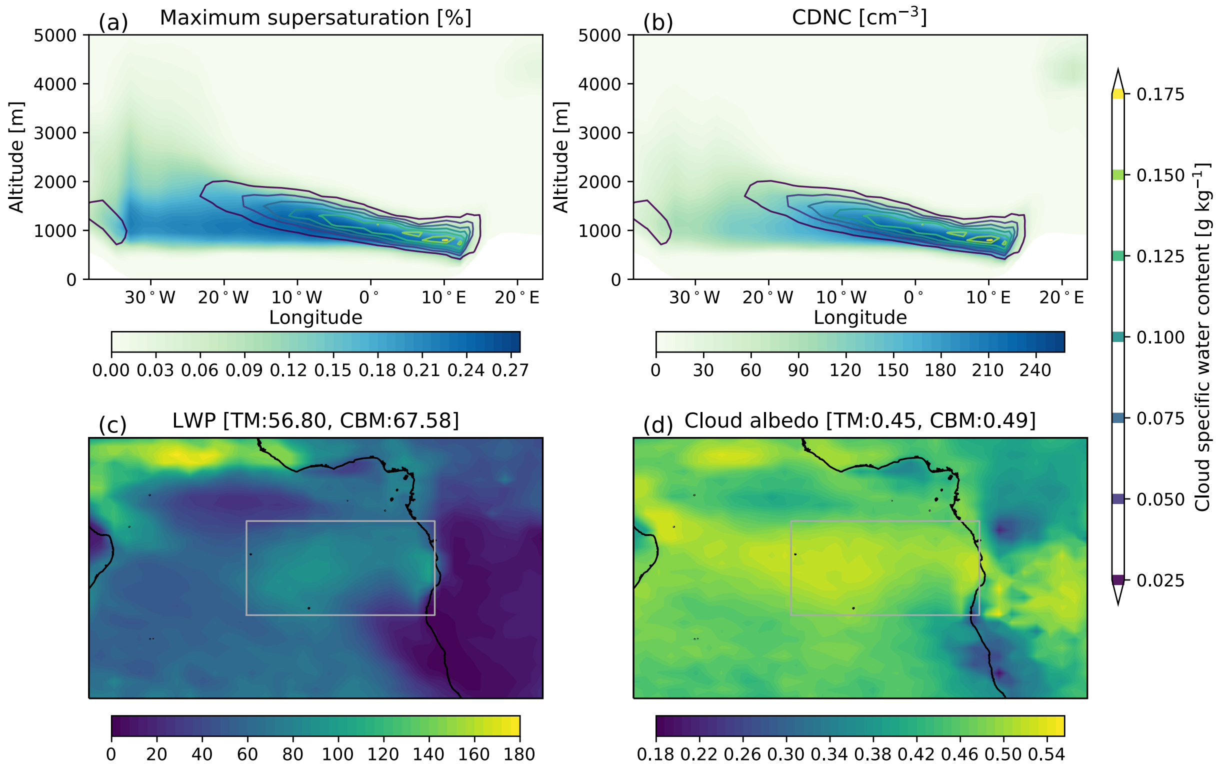

Figure 3. UKESM1 simulated mean (a) vertical profiles of maximum supersaturation and (b) vertical profiles of cloud droplet number concentration along the latitude of Ascension Island; spatial distribution of (c) cloud liquid water path and (d) cloud albedo from the International Satellite Cloud Climatology Project (ISCCP) simulator. These means are averaged during July and August, 2016-2017. The contour lines in (a-b) are the cloud specific water content. The TM in (c-d) is the total mean of the domain, and the CBM is the mean of the cloud box (the grey box on the map) representing the areas where the average low cloud fraction is above 0.58.

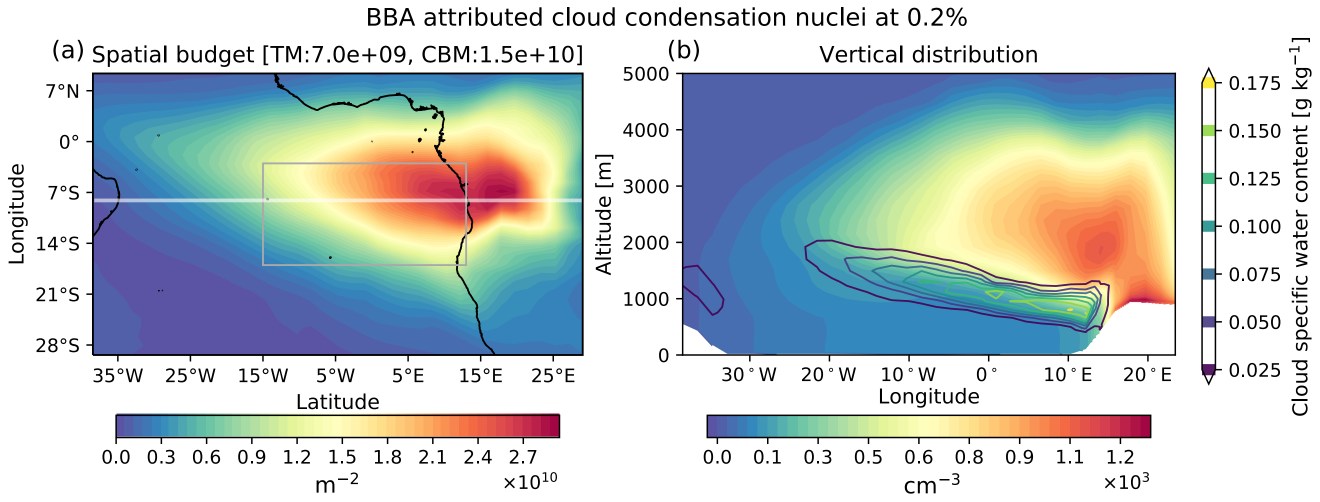

Figure ~~3~~4. UKESM1 simulated mean cloud condensation nuclei attributed to BBA at 0.2% supersaturation under standard conditions for temperature and pressure (STP) during July and August 2016-2017 as (a) the vertically integrated burden and (b) profile along the latitude of Ascension Island, 8.1° S (the white line in ~~Fig.~~Fig. 3a). The domain in ~~Fig.~~Fig. 3a, ranging from 30° S to 10° N and from 40° W to 30° E, is the areas this paper interested in. The grey box in the map (cloud box) representing the cloud areas where the averaged low cloud fraction is above 0.58. The TM is the total mean of the domain and the CBM is the mean of the cloud box. The contours in ~~Fig.~~Fig. 3b are the cloud specific water content in the baseline simulation.

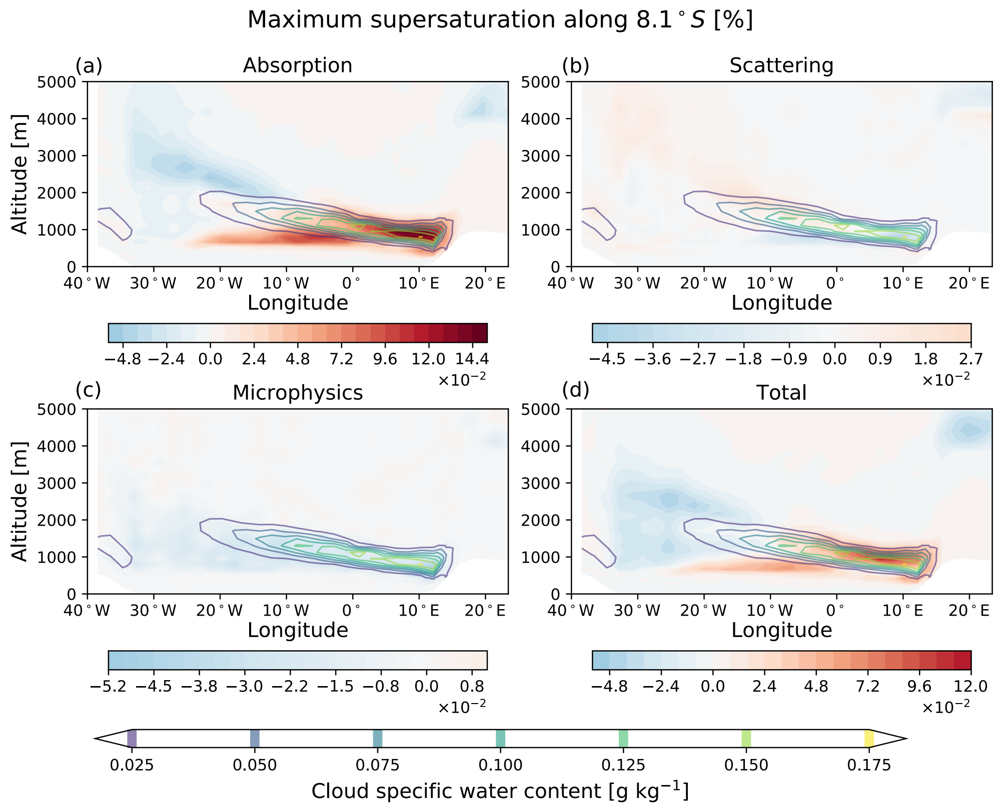

Figure 45. UKESM1 simulated mean vertical profiles of the BBA effects (a) absorption, (b) scattering, (c) microphysical and (d) total on maximum supersaturation along the latitude of Ascension Island (cf. ~~Fig.~~Fig. 3a) during July and August, 2016-2017. The contour lines are the baseline cloud specific water content. The same colourmap scale is used in each plot to facilitate comparison, but the colourmap ranges differ in each plot, corresponding to the maximum and minimum of SS at each.

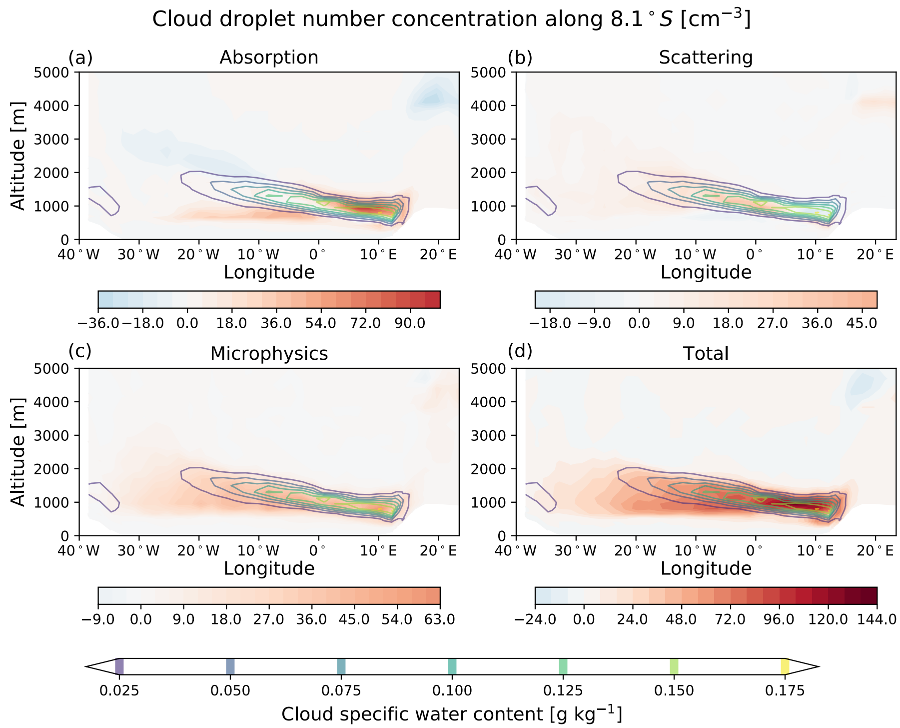

Figure ~~5~~6. Same as ~~Figure~~Fig. 4 but for the in-cloud cloud droplet number concentration per cubic centimetre.

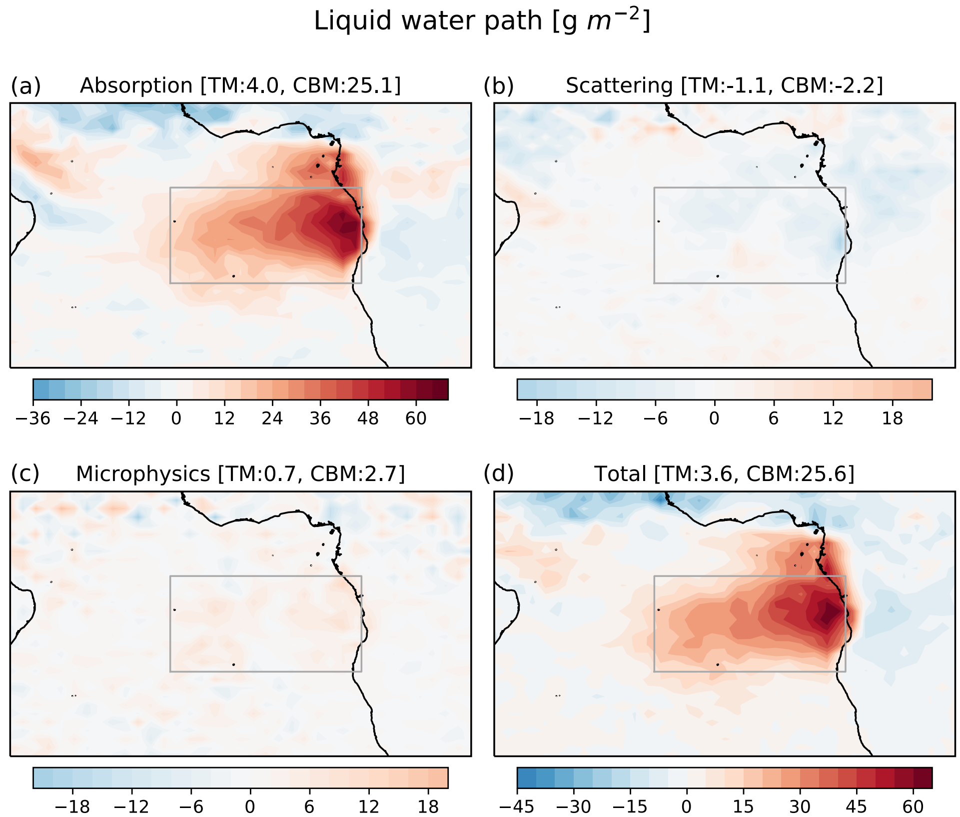

Figure ~~6~~7. UKESM1 simulated mean spatial distribution of the BBA effects of (a) absorption, (b) scattering, (c) microphysical and (d) total on the cloud liquid water path during July and August, 2016-2017. The domain range is from 30° S to 10° N, and from 40° W to 30° E. The TM is the total mean of the domain and the CBM is the mean of the cloud box (the grey box on the map) representing the areas where the average low cloud fraction is above 0.58. The same colour scale is used in each plot to facilitate comparison, but the colourmap ranges differ in each plot, corresponding to the maximum and minimum variation of LWP in each.

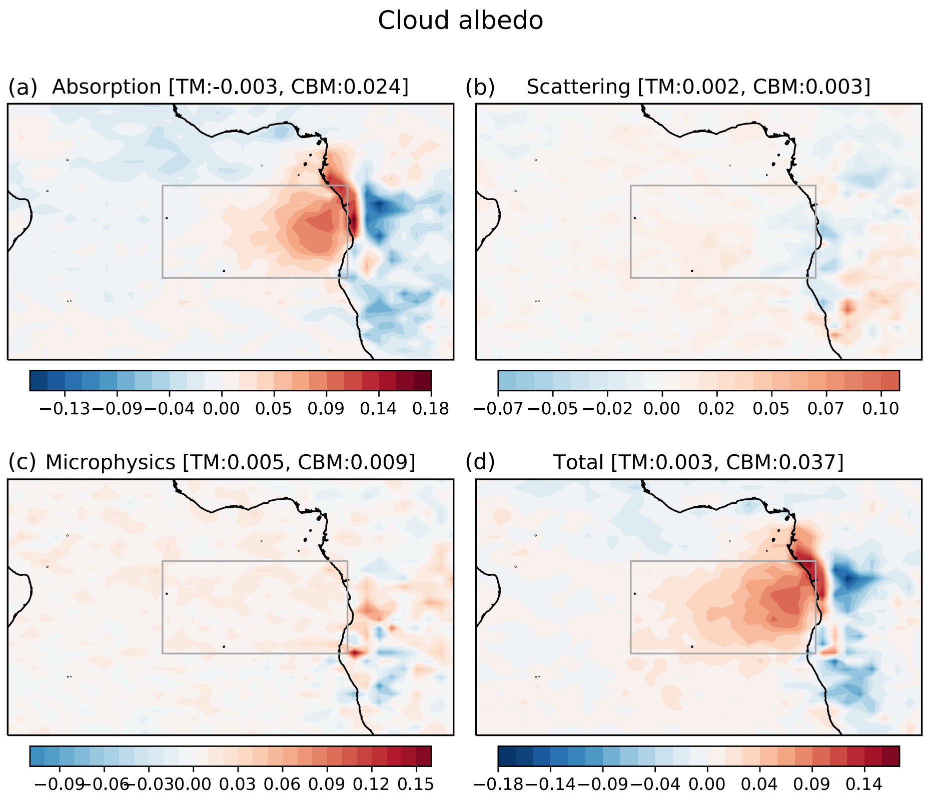

Figure ~~7~~8. UKESM1 International Satellite Cloud Climatology Project (ISCCP) simulator mean spatial distribution of the BBA effects of (a) absorption, (b) scattering, (c) microphysical and (d) total on the cloud albedo during July and August, 2016-2017. The domain range is from 30° S to 10° N, and from 40° W to 30° E. The TM is the total mean of the domain and the CBM is the mean of the cloud box (the grey box on the map) representing the areas where the average low cloud fraction is above 0.58. The same colour scale is used in each plot to facilitate comparison, but the colourmap ranges differ in each plot, corresponding to the maximum and minimum variation of cloud albedo in each.

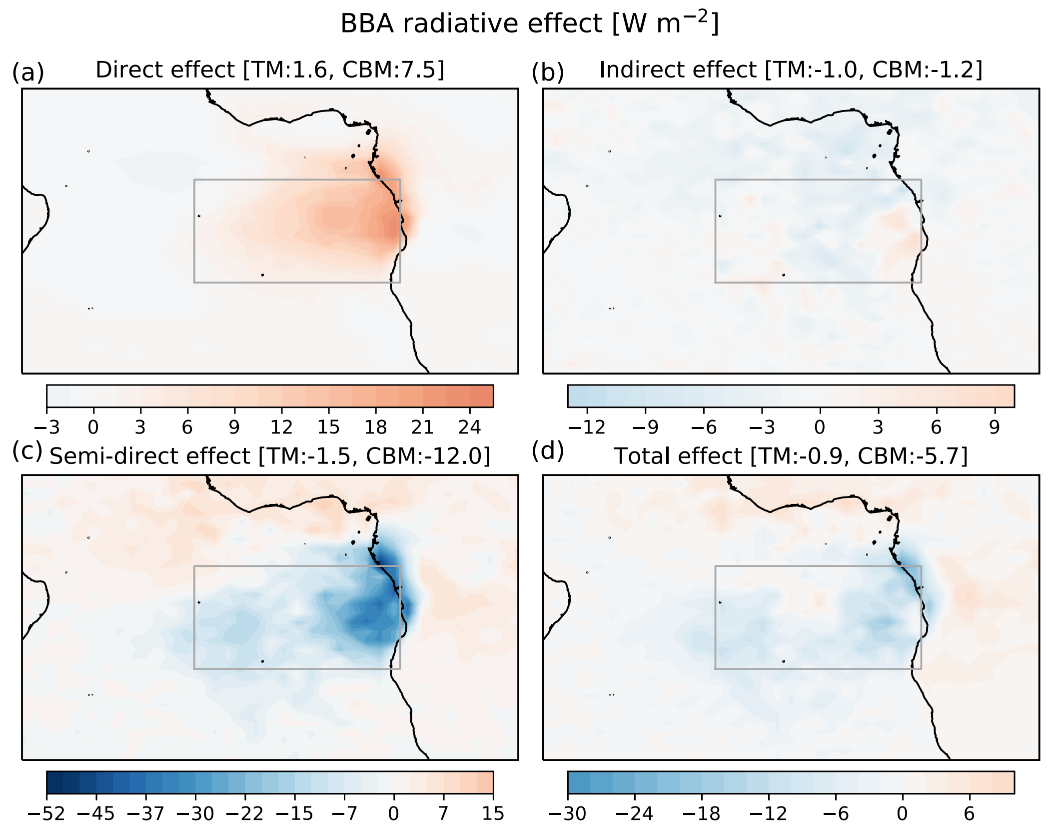

Figure ~~8~~9. UKESM1 mean net (shortwave + longwave) biomass burning aerosols (a) Direct, (b) indirect, (c) semi-direct, and (d) total radiative effects during July and August, 2016-2017. The same colourmap scale is used for each plot, but the colourmap ranges differ in each plot, corresponding to the maximum and minimum of the effect in each.

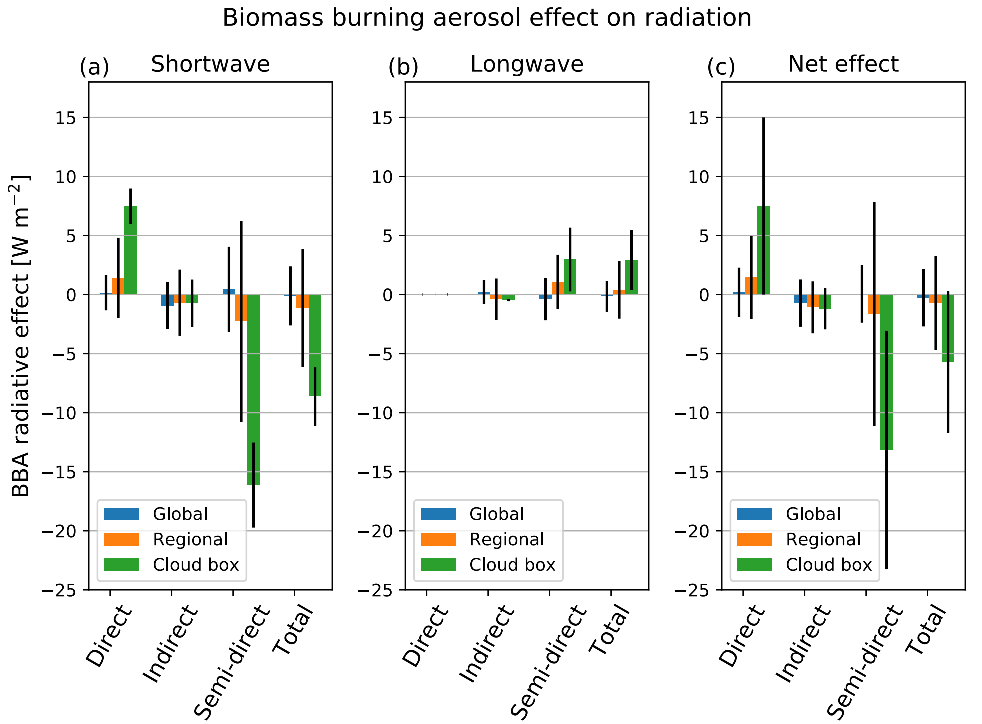

Figure ~~9~~10. Bar chart of UKESM1 mean BBA radiative effect during July and August, 2016 to 2017. The BBA radiative effect at (a) shortwave, (b) longwave, and the (c) net effect are presented in separate plots. The blue colour represents the global mean, the orange is the domain mean, and the green is the cloud box mean. The error bars represent standard errors.